Improved multi-objective Jaya optimization algorithm for a solar dish Stirling engine

Cite as: J. Renewable Sustainable Energy **11**, 025903 (2019); https://doi.org/10.1063/1.5083142
Submitted: 28 November 2018 . Accepted: 11 January 2019 . Published Online: 15 March 2019

R. Venkata Rao, Hameer Singh Keesari, P. Oclon, and Jan Taler

Journal of Renewable and Sustainable Energy ARTICLE scitation.org/journal/rse

Improved multi-objective Jaya optimization algorithm for a solar dish Stirling engine

Cite as: J. Renewable Sustainable Energy **11**, 025903 (2019); doi: 10.1063/1.5083142
Submitted: 28 November 2018 · Accepted: 11 January 2019 · Published Online: 15 March 2019

R. Venkata Rao,[1,a)] Hameer Singh Keesari,[1] P. Oclon,[2] and Jan Taler[2]

AFFILIATIONS

[1]Department of Mechanical Engineering, Sardar Vallabhbhai National Institute of Technology, Surat 395007, India
[2]Institute of Thermal Power Engineering, Politechnika, Krakowska, Krakow, Poland

[a)]Author to whom correspondence should be addressed: ravipudirao@gmail.com

ABSTRACT

This study proposes an adaptive multi-team perturbation guiding Jaya (AMTPG Jaya) algorithm. The proposed approach uses multiple teams to explore the search space. Depending on the percentage of consumed function evaluations, the AMTPG Jaya algorithm adjusts the number of teams in the search. Furthermore, all teams move from a single population set and are simultaneously guided by different perturbation equations to different regions of search space. As each team has a different perturbation scheme, the set of moves to new positions by each team is unique. During the search process, the perturbation equations are exchanged depending on the quality of the solutions produced by them. The proposed algorithm employs dominance principles and the crowding distance estimation method to handle the multiple objectives simultaneously. The proposed algorithm is examined using two multi-objective optimization case studies of a solar dish Stirling heat engine system and a multi-objective optimization case study of the Stirling heat pump. Also, the Technique for Order of Preference by Similarity to Ideal Solution decision-making method is employed for identifying an optimal solution. The computational results obtained by the proposed AMTPG Jaya algorithm are superior to those achieved by the other algorithms presented in this work.

I. INTRODUCTION

Global warming is a substantial issue that requires cleaner production of energy. Renewable energy resources are significant sources of contribution for such clean energy demands. Taking advantage of these renewable energy sources provides significant opportunities for handling energy-related problems. Solar power is a low-grade renewable energy resource which is vastly available. The solar dish Stirling heat engine (SDSHE) contains a solar-powered heat engine which extracts heat energy from sun rays and converts that into useful energy. Because of the high capability of recuperating low-grade heat with possibly high efficiencies, Stirling cycle engines have attracted growing attention over the past few decades. Due to the growth of the fuel crisis, Stirling engines have become a viable proposition with quick advances in technology.[37] For converting the heat energy into useful mechanical work, this cycle works on the principle of periodic compression and expansion of working fluid at different temperature levels. Tlili *et al.*[38] researched an irreversible Stirling heat engine model taking air as the working fluid and illustrated the effect of internal irreversibility on the operating temperature and overall efficiency of the system. Blank *et al.*[8] analyzed an endo-reversible Stirling engine with external heat transfer irreversibility by employing finite time thermodynamics (FTT) to obtain maximum power and efficiency. Kaushik and Kumar[14,15] formulated a Stirling heat pump and engine model considering finite heat capacity and heat leak between external heat reservoirs and losses of internal heat energy in the regenerator.

Several researchers had investigated the optimization of SDSHE performance. Sharma *et al.*[35] investigated the performance of an SDSHE system and demonstrated the effect of heat reservoir temperatures to obtain higher power output and the corresponding thermal efficiency. Yaqi *et al.*[42] formulated a mathematical model using FTT to obtain the overall thermal efficiency for an SDSHE system with finite regeneration process time, thermal bridging losses, finite-rate heat transfer, and regenerative heat losses. Furthermore, the authors had studied the effect of the absorber temperature, concentrating ratio, heat leak coefficient, and effectiveness of the regenerator by keeping the other parameters constant and found that the optimum concentrating ratio was 1300 and the temperature of the absorber was 1100 K. Ahmadi *et al.*[4] extended the work of Yaqi *et al.*[42] by simultaneously optimizing the output power and thermal efficiency by employing multi-objective optimization through a non-dominated sorting genetic algorithm (NSGAII) to an SDSHE with imperfections in the performance of the collector. The authors had presented the

effects of variation in the system parameters such as the solar flux intensity, volumetric ratio, dish concentration ratio, effectiveness of the regenerator, and conductive bridge losses. Toghyani *et al.*[39] studied the effect of pressure drop in the heat exchangers on efficiency and power of a Stirling engine by nonideal adiabatic analysis and identified the optimum design parameters using NSGAII. Ahmadi *et al.*[5] simulated the effects of the system parameters of an SDSHE system on the output power, the rate of entropy generation, and thermal and exergetic efficiencies by maximizing the output power with respect to the maximum temperature of the working medium in the Stirling cycle. They found that the regenerator effectiveness had a threshold value below which the entropy generation rate was independent of regenerator effectiveness. Also, maximum thermal and exergetic efficiencies were observed at absorber temperatures of 900 K and 800 K, respectively. Liao and Lin[16] determined maximum power and the consequent optimal efficiency of an SDSHE using the Lagrange multiplier method and irreversible thermodynamics and found that the decrease in the sink temperature and the heat leak coefficient can lead to improved system performance.

Several researchers had studied multi-objective optimization of SDSHE systems using various algorithms such as NSGAII, the Multi-objective particle swarm optimization (MOPSO) algorithm, the improved multi-objective bare-bone particle swarm optimization (IMOBBPSO) algorithm, Front-based Yin-Yang-Pair Optimization (FYYPO), and the Grey Wolf Optimization (GWO) Algorithm. Ahmadi *et al.*[1] employed the NSGA-II algorithm to find the optimal parameters for two multi-objective optimization scenarios of an SDSHE system; the first was to maximize the power output, entransy loss rate, and thermal efficiency simultaneously; the second was to simultaneously maximize the entransy loss rate and power output and minimize the rate of entropy generation. Arora *et al.*[6] performed multi-objective optimization of the thermal efficiency, ecological function, and power output of an SDSHE using the NSGA-II algorithm. In another work, Arora *et al.*[7] employed the NSGA-II algorithm to identify the optimal parameters of the SDSHE system which simultaneously optimizes the thermoeconomic function, thermal efficiency, and power output. Hooshang *et al.*[13] employed the NSGA-II algorithm for multi-objective optimization of power output and regenerator pressure. Duan *et al.*[12] employed the MOPSO algorithm for simultaneous maximization of thermal efficiency of the SDSHE system, irreversibility parameter of the cycle, and power output. Nazemzadegan *et al.*[18] implemented the MOPSO algorithm for simultaneous optimization of four objectives which include thermal efficiency, dimensionless power, economic factor, and entropy. Niu *et al.*[19] proposed the IMOBBPSO algorithm for two objective simultaneous optimization which included minimization of entropy generation and maximization of power output. The FYYPO algorithm was employed by Punnathanam and Kotecha[21] for simultaneous optimization of two scenarios of the SDSHE system. Tavakolpour-Saleh *et al.*[36] proposed the GWO algorithm for simultaneous optimization of the efficiency of the system, power output, and pressure loss of the Stirling heat engine.

From the above literature, it can be inferred that various researchers had proposed different optimization techniques considering different performance criteria of the SDSHE system for multi-objective optimization of an SDSHE system. In the present work, two case studies of an SDSHE system and a case study of a Stirling heat pump have been considered for multi-objective optimization using an improved version of the Jaya algorithm. Rao[24] had proposed the Jaya algorithm that has no algorithmic constraints. The performance of the Jaya algorithm had been validated using different optimization benchmark functions and engineering applications[25] such as the structural damage identification problem,[11] micro-channel heat sink application,[28] shell and tube heat exchanger application,[32] plate-fin heat exchanger application,[34] image detection application,[40] network power flow application,[41] and tea-category identification using image detection application.[44] Michailidis[17] proposed the hybrid parallel Jaya algorithm called the HHCPJaya algorithm for large-scale global optimization problems in the multi-core environment. Rao *et al.*[31] proposed the multi-objective Jaya algorithm for simultaneous optimization of advanced machining processes' aspects. Rao *et al.*[27] proposed a self-adaptive Jaya algorithm for simultaneous optimization of multiple objectives of a Stirling heat engine. Rao and Saroj[33] proposed an elitist-Jaya algorithm for simultaneous optimization of multiple objectives of heat exchangers. Rao and Keesari[26] proposed the multi-team perturbation guided Jaya (MTPG Jaya) algorithm for wind farm layout optimization. In this variant of Jaya algorithm, the authors had introduced a multi-population concept with adaptive perturbation, which uses six-movement equations to aid the multiple populations in exploring the search space. In the MTPG Jaya algorithm, the population size and the number of teams need to be tuned according to the optimization problem. However, as the complexity of the problem increases, tuning of the population size and number of teams concurrently can become a tiresome work. Also, the MTPG Jaya algorithm uses stagnation treatment which includes the probability of accepting worst solutions (P_a) and criterion for stagnation. These parameters required tuning and may make the algorithm time-consuming. Thus, in this work, the multi-objective optimization variant of the MTPG Jaya algorithm which adapts the number of teams has been proposed to handle the SDSHE system case studies. The contributions of this work are:

- The multi-objective optimization adaptive multi-team perturbation guiding Jaya (AMTPG Jaya) algorithm has been proposed, in which a single population set is simultaneously guided by selected perturbation or movement equations to different regions of search space. Furthermore, the proposed algorithm adapts the number of teams based on the function evaluations consumed and exchanges the movement equation based on the quality of the solutions produced.
- The performances of Jaya, MTPG Jaya, and AMTPG Jaya algorithms have been investigated using two multi-objective optimization case studies of the SDSHE system and a multi-objective optimization case study of the Stirling heat pump.
- The Technique for Order of Preference by Similarity to Ideal Solution (TOPSIS) decision-making method has been employed to compare the performance of the proposed algorithm with other algorithms reported in the literature.

Section II presents the working principle of the proposed algorithm.

II. ADAPTIVE MULTI-TEAM PERTURBATION GUIDING JAYA ALGORITHM

In the proposed AMTPG Jaya algorithm, only one set of population is used for the search process. The single population set is simultaneously guided by selected perturbation or movement equations to different regions of search space. This movement of the population

through one movement equation is considered as a team in this work. Each team has an equal probability of selecting a movement equation from the available movement equations. Depending on the available number of function evaluations, the proposed algorithm adapts the number of teams. The movement equations considered here are the well-established variations of the Jaya algorithm equation including the Jaya algorithm equation.[20,24,29,43] Before the beginning of the search process, the number of teams to explore is selected randomly, and each team is assigned with a movement equation randomly. These movement equations guide the population towards distant regions of the search space. Each team moves the population uniquely as they have different movement equations and corresponding random numbers. Also, the movement equation of the worst performing team (the team with a higher violation value) is substituted with any other movement equation randomly. Furthermore, the proposed algorithm follows the posteriori approach to handle more than one objective simultaneously. The proposed algorithm ranks the candidate solutions according to the dominance principles and crowding distance estimation method.[10,30] The candidate solution that has the best rank value (i.e., 1) and maximum crowding distance (ξ) is considered to be the best candidate. On the other hand, the solution having the worst rank value and lowest ξ value is considered as the worst solution. Such a selection scheme is adopted so that the solution in the less populous region of the objective space may guide the search process.

Let an objective function, independent of the D number of design variables (i.e., $v = 1, 2 \ldots D$), be G(u). According to the basic Jaya algorithm, the set of a random population of size N (i.e., $p = 1, 2 \ldots N$) is updated by[24]

$$u'_{v,p,i} = u_{v,p,i} + r_{1,v,i}\left(u_{v,\text{best},i} - |u_{v,p,i}|\right) - r_{2,v,i}\left(u_{v,\text{worst},i} - |u_{v,p,i}|\right), \tag{1}$$

where, during the ith iteration for the vth variable, $u_{v,p,i}$ is the value for the pth candidate in the population, $u_{v,\text{best},i}$ is the value for the best candidate solution, $u_{v,\text{worst},i}$ is the value for the worst candidate solution, and $u'_{v,p,i}$ is the updated value of $u_{v,p,i}$. Similarly, $r_{1,v,i}$ and $r_{2,v,i}$ are the two random numbers selected from a uniform distribution in the range [0, 1] for the v^{th} variable in the ith iteration. In Eq. (1), the term $r_{1,v,i}\left(u_{v,\text{best},i} - |u_{v,p,i}|\right)$ indicates the movement of the current candidate solution towards the best solution. The amount of movement is controlled by the random number $r_{1,v,i}$. Similarly, the term $-r_{2,v,i}\left(u_{v,\text{worst},i} - |u_{v,p,i}|\right)$ indicates the movement of the current candidate solution to avoid the worst solution and the amount of movement is controlled by the random number $r_{2,v,i}$. If the updated solutions have better fitness than the respective old solutions, then the respective updated solutions are accepted; otherwise rejected. Then the updated population is moved to the subsequent iterations. This procedure is repeated till the termination criterion is met. For more details about the working of the Jaya algorithm and sample codes of constrained and unconstrained optimization problems, the readers may refer to Rao.[23]

The movement equations considered for the proposed algorithm are presented in Eqs. (1)–(9). Equation (2) is similar to that of the Jaya algorithm movement equation in which the two random numbers are replaced by two chaotic-random numbers (C_m) to guide the movement of the solution. Equation (3) presents the method of generating Chaotic-random numbers and this chaotic sequence features randomicity and ergodicity which will further enhance the capability to escape from the local optima[43]

$$u'_{v,p,i} = u_{v,p,i} + c_{m1,v,i}\left(u_{v,\text{best},i} - |u_{v,p,i}|\right) - c_{m2,v,i}\left(u_{v,\text{worst},i} - |u_{v,p,i}|\right), \tag{2}$$

$$c_{m+1} = 4c_m(1 - c_m). \tag{3}$$

Equation (4) is a quasi-opposition movement equation.[29] The quasi-opposition movement is introduced to diversify the population further and to improve the convergence rate of the proposed algorithm. This quasi-opposition movement simultaneously considers the candidate solutions opposite to the current candidate solutions. Let the lower and upper bounds of a variable v be LB_v and UB_v, respectively, then the quasi-opposite value of the candidate solution variable $u_{v,p,i}$ is given by

$$u^q_{v,p,i} = rand(a, b), \tag{4}$$

where

$$a = \frac{\text{LB}_v + \text{UB}_v}{2}, \tag{5}$$

$$b = \text{LB}_v + \text{UB}_v - u_{v,p,i}. \tag{6}$$

Equation (7) presents the fourth movement equation considered in this work.[20] The working principle of this movement is comparable to that of the Jaya algorithm, but in place of the best candidate solution, any one of the top three solutions ($rb \in \{1, 2, 3\}$) is selected arbitrarily. The multiple best candidates approach will enhance the capability of scanning of the search domain.

$$u'_{v,p,i} = u_{v,p,i} + r_{1,v,i}\left(u_{v,\text{best}(rb),i} - |u_{v,p,i}|\right) - r_{2,v,i}\left(u_{v,\text{worst},i} - |u_{v,p,i}|\right). \tag{7}$$

The next movement equation is given by Eq. (8).[43] Let *rand* be a uniformly distributed random number between [0, 1]. Then, the updated solution is now produced using Eq. (8). This chaotic movement mechanism will further improve the quality of one solution by generating a new solution around it

$$u'_{v,p,i} = u_{v,\text{best},i} + rand(2c_m - 1). \tag{8}$$

The next movement equation is given by Eq. (9), which is the same equation as the previous movement equation in which a random number in the range [0, 1] substitutes the chaotic-random number

$$u'_{v,p,i} = u_{v,\text{best},i} + rand(2rand - 1). \tag{9}$$

Team violation is calculated based on the variable boundary violations using Eq. (10). The team (T) violations are calculated for all $u_{v,p,i,T} < \text{LB}_v$ or $u_{v,p,i,T} > \text{UB}_v$

$$Violation_T = \sum_{p=1}^{N}\sum_{v=1}^{D}\left|u_{p,v,i,T} - \text{UB}_v\right| + \left|\text{LB}_v - u_{p,v,i,T}\right|. \tag{10}$$

If $u_{v,p,i} < \text{LB}_v$, then it is taken as LB_v.
If $u_{v,p,i} > \text{UB}_v$, then it is taken as UB_v.

A. Ranking based on non-dominance principles

Let N be a set of candidate solutions to be ranked for an optimization problem consisting of M number of objectives. For a minimization objective, a candidate solution x_k is considered as dominating another candidate solution x_l if and only if $G_j(x_k) \leq G_j(x_l)\ \forall\ 1 \leq j \leq M$

and $G_j(x_k) < G_j(x_l)$ for at least one j, where $j \in \{1,2,\ldots M\}$. A candidate solution x_k in population N is considered as a non-dominated candidate if there is no candidate solution x_l in population N which dominates x_k. In this manner, every candidate solution in N is compared with other candidate solutions in N, and the non-dominated candidates are ranked one. The remaining (excluding the ranked candidates) candidates are also ranked in the same manner and ranked two. This procedure is continued until all the candidate solutions are ranked. All the candidate solutions with the same rank will be considered as the front (F).

B. Crowding distance (ξ) calculation

The crowding distance (ξ_k) is an approximate concentration of the candidate solutions in the neighbourhood of a particular candidate solution k. For a selected front F, the number of solutions in front $l = |F|$ is determined and $\xi_k = 0 \; \forall \; k \in l$ is assigned. Then for each objective function $j = 1,2,\ldots M$, the set is sorted in the worst order of G_m. The largest crowding distance is assigned to boundary solutions in the sorted list ($\xi_1 = \xi_l = \infty$), and for all the other candidates in the sorted list $k = 2$ to $(l-1)$, the crowding distance is assigned as follows:

$$\xi_k = \xi_k + \left(G_j^{k+1} - G_j^{k-1}\right) / \left(G_j^{max} - G_j^{min}\right), \tag{11}$$

where G_j is the objective function value of the jth objective and $G_j^{\max}$ and $G_j^{\min}$ are the population-maximum and population-minimum values of the jth objective function.

In the multi-objective optimization cases, more than one optimal candidate solution exists. Thus, to find efficient Pareto-frontier using the proposed algorithm a candidate from the remote area of the search area is given more priority than the candidate in the packed area of the search area. In the proposed algorithm, the candidate having better rank is given higher priority, and among the two competing candidates having equal rank, the solution with a higher ξ value is preferred. This will avoid converging towards a single optimum candidate solution and ensure diversity among the candidate solutions.

C. Steps in the AMTPG Jaya algorithm

The flowchart of the AMTPG Jaya algorithm is shown in Fig. 1. The stepwise procedure of the AMTPG Jaya algorithm is as follows:

Step 1: Initialize control parameters such as N (size of population), NT (No. of teams), D (No. of variables), LB (Lower boundary), UB (Upper boundary), $MaxMI$ (The number of iterations allowed after assigning perturbation equations to teams), and Termination criteria.
Step 2: Evaluate the initial population and rank the candidate solutions according to the dominance principles and crowding distance.
Step 3: Assign perturbation equations randomly for each team. Start the counter for movement iterations (MI).
Step 4: Update the population of each team using the perturbation equation assigned to them. Calculate the boundary violations for each team.
Step 5: Evaluate the population of each team and find the fitness values. For each candidate solution, rank the teams using the ranking scheme as explained earlier. To rank teams, all the candidate solutions ($j = 1,2,3\ldots N$) of teams are compared with the respective candidate solutions. After assigning ranks to each team concerning each candidate solution, calculate the average ranks for each team.
Step 6: Update the population. First, for each candidate solution ($j = 1,2,3\ldots N$), select the best candidate solution from the respective candidate solutions of each team ($k = 1,2,3\ldots NT$). Then add the previous population to the updated population. Rank the candidate solutions of the previous and updated population together according to the dominance principles and crowding distance. Select N best candidates having best rank values and highest crowding distance.
Step 7: Calculate the quality of the teams; the quality of team i is given by $TQ_i = ATR_i + TV_i$, Where ATR_i and TV_i are ith team average rank and boundary violation, respectively. The team, having less TQ value considered as the best team and the team that has more TQ value considered as the worst team. The TQ values are calculated in all the iterations and accumulated until MI reaches $MaxMI$. When MI=$MaxMI$, replace the worst team perturbation equation arbitrarily with other than the current perturbation equation and set $MI = 0$.
Step 8: Update the number of teams. The proposed approach updates the number of teams based on the number of function evaluations completed. Initially, the search starts with a maximum number of teams. As the search progresses, the number of teams is randomly either reduced or increased by one for every time $MI = MaxMI$. After completing 60% of function evaluations, the number of teams is reduced by one whenever $MI = MaxMI$ and maintained a minimum number of teams. After updating the number of teams, it allows the teams to explore and exploit search space until MI reaches $MaxMI$.
Step 9: Check the termination criteria. In the event, the search process satisfies the termination criteria then stop the algorithm and report the final set of the population, else start the next iteration from **Step 4**.

Generally, the number of function evaluations is taken as the algorithm computational expenditure. Let TI be the total number of iterations, then, the computational expense of the AMTPG Jaya algorithm can be calculated by $N \times NT \times TI$. However, the number of teams of the AMTPG Jaya algorithm will be varying as the search process is in progress. Thus, in the computational experiments, computational expense in iterations can be calculated by multiplying the number of population with the number of teams in the respective iteration and the summation of computational expense of all iterations will give the total computational expense. The proposed AMTPG Jaya algorithm is now tried on multi-objective optimization case studies of the SDSHE system and a Stirling heat pump. Section III presents a brief description of the SDSHE system and the Stirling heat pump.

III. SYSTEM DESCRIPTION

A. SDSHE system

The solar dish Stirling heat engine (SDSHE) system consists of a solar-powered heat engine which extracts the heat energy from sun rays and converts that into useful energy. This heat engine works based on the Stirling cycle. The warm region of the Stirling engine is placed at the focal point of the concentrator. The concentrator reflects the solar energy towards the focal point. The heat exchanger placed at the warm region of the Stirling engine transmits this reflected heat energy to the working fluid. The work output from the Stirling cycle is then utilized to drive a generator that produces electric power.

The Stirling cycle (with ideal regenerator) consists of four processes as shown in Fig. 2. Process 1–2: an isothermal (at T_c temperature) compression involving heat rejection to the heat sink (at T_L temperature). Process 2–3: an isochoric (volume $V_2 = V_3$) heating process, in which the temperature of the working fluid raises to T_h by the regenerator. Process 3–4: an isothermal (at T_h temperature) expansion process, in which heat added to the working fluid from the heat source (at T_H temperature). Process 4–1: an

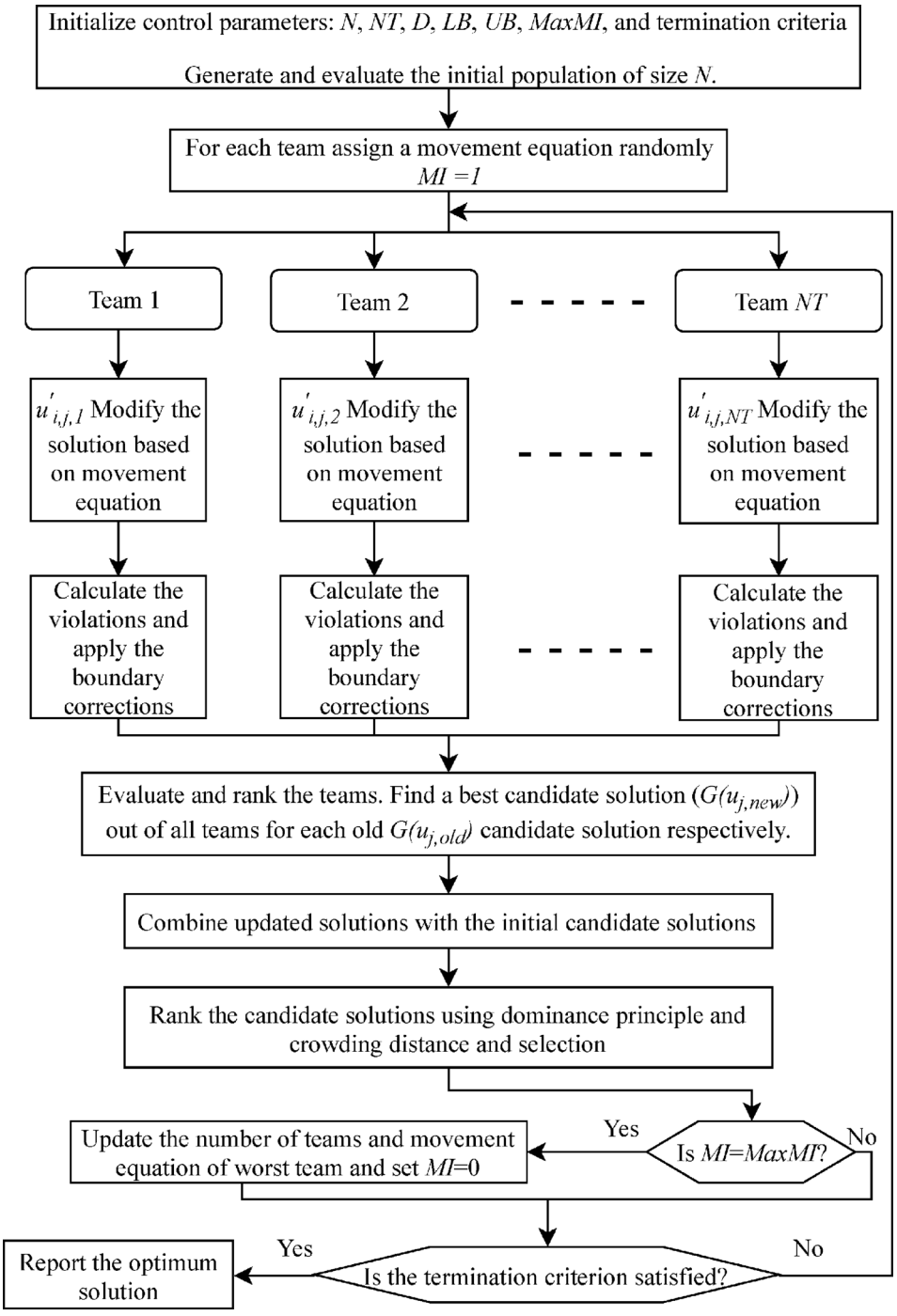

FIG. 1. Flowchart of the AMTPG Jaya algorithm.

isochoric (volume $V_4 = V_1$) process, in which the regenerator absorbs heat from the working fluid, and thus, temperature falls from T_h to T_c. In the present work, two multi-objective optimization case studies of an SDSHE system are considered. Detailed description and FTT analysis of these case studies were presented by Ahmadi *et al.*[3] and Dai *et al.*,[9] respectively.

B. Stirling heat pump

The Stirling heat pump works on the reverse Stirling cycle which consists of two isothermal and two isochoric processes as shown in Fig. 3. Process 1–2: isothermal (at $T_c = T_1 = T_2$) expansion process in which the working fluid absorbs heat (Q_L) from the heat source (T_L). Process 2–3: an isochoric process in which the working fluid absorbs

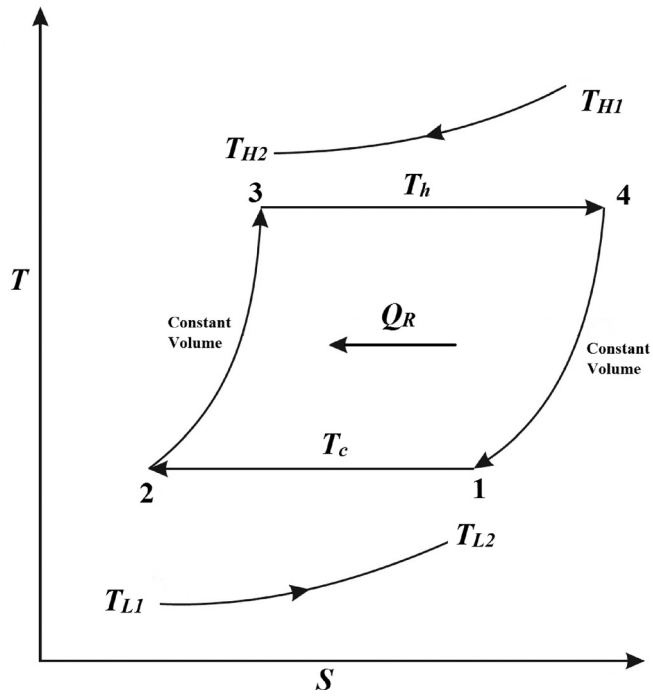

FIG. 2. T-S diagram of the Stirling heat engine cycle.

heat (Q_R) from the regenerator and attains maximum temperature ($T_h = T_3 = T_4$). Process 3–4: isothermal compression (at $T_h = T_3 = T_4$) in which working fluid rejects heat (Q_H) to the heat sink (T_H). Process 4–1: an isochoric process in which the working fluid rejects heat (Q_R) to the regenerator and attains minimum temperature ($T_c = T_1 = T_2$) in the cycle.

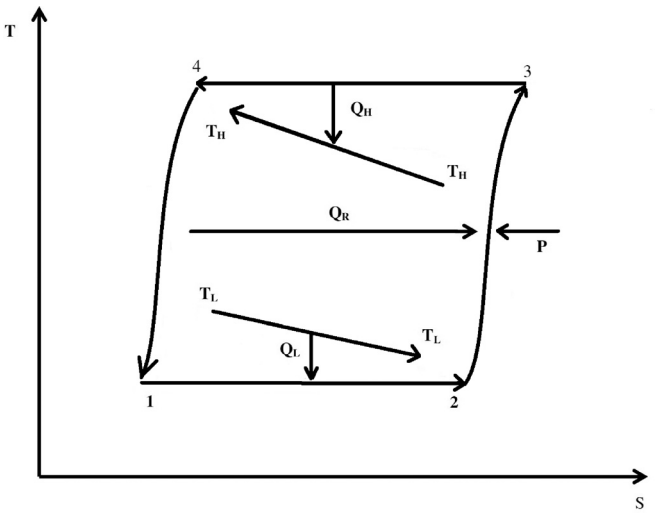

FIG. 3. T-S diagram of the Stirling heat pump cycle.

A multi-objective optimization case study of an irreversible Stirling heat pump is considered in this case study for determining the optimal design parameters which simultaneously optimizes the input power, the heating coefficient of performance, and the heating load. Detailed description and thermodynamic analysis of this case study were presented by Ahmadi *et al.*[2] Section IV presents the multi-objective optimization case studies and the associated computational results obtained by the proposed algorithm.

IV. MULTI-OBJECTIVE OPTIMIZATION CASE STUDIES AND COMPUTATIONAL RESULTS

The multi-objective optimization problem deals with the simultaneous optimization of more than one objective while satisfying several constraints. The difficulty with these problems is that the trade-offs between the objectives are not known, and there is no single candidate solution vector which will optimize all the objectives of the problem, i.e., conflicting objectives. Thus, in optimizing these problems, the Pareto optimal solution method is employed. A candidate solution is the Pareto optimal solution if there is no candidate solution dominating it.

In this work, two multi-objective optimization case studies of an SDSHE system and a case study of the Stirling heat pump are considered for execution and justification of the proposed algorithm. These case studies have been taken from Ahmadi *et al.*[2,3] and Dai *et al.*[9] The computational experiments for these case studies are carried out by the AMTPG Jaya, MTPG Jaya, and Jaya algorithms. The posteriori approach[10,30,31] is used for simultaneous optimization of the multiple objectives. The Pareto optimal solutions obtained by the algorithms are non-dominated solutions. Therefore, to facilitate the comparison between the algorithms, a final optimal solution is selected using the TOPSIS[22] decision-making method. The TOPSIS method provides the relative similarity index (SI) based on selected ideal (O_j^{ideal}) and non-ideal (O_j^{nonideal}) solutions. The ideal and non-ideal solutions represent the hypothetical best and worst scenarios of all the objectives, respectively. Let O_{ij} be the normalized value of the jth objective for the ith candidate solution in a Pareto frontier, then the distance (d_i) of each Pareto optimal from the ideal and non-ideal solution can be calculated by using the following equations, respectively,

$$d_i^{ideal} = \sqrt{\sum_{j=1}^{M} \left(O_{ij} - O_j^{ideal}\right)^2}, \tag{12}$$

$$d_i^{nonideal} = \sqrt{\sum_{j=1}^{M} \left(O_{ij} - O_j^{nonideal}\right)^2}, \tag{13}$$

where $i = 1, 2, \ldots N$ (i.e., the number of Pareto optimal candidate solutions in a Pareto frontier) and $j = 1, 2, \ldots M$ (i.e., the number of objectives of the Pareto frontier). In all the computations of these case studies, the Euclidian–normalization method has been employed, which is given by the following equation:

$$O_{ij} = G_{ij} \Big/ \sqrt{\sum_{i=1}^{N} \left(G_{ij}^2\right)}. \tag{14}$$

Now, the similarity index can be calculated using the following equation:

$$SI = \frac{d_i^{nonideal}}{d_i^{ideal} + d_i^{nonideal}}. \quad (15)$$

If the similarity index of a Pareto optimal solution is higher than that of all other solutions in the Pareto-frontier, then it is the nearest solution to the ideal solution. Similarly, if the similarity index of a Pareto optimal solution is lower than that of other solutions in the Pareto-frontier, then it is the nearest solution to a non-ideal solution. For more details about the TOPSIS method, the readers may refer to Rao.[22] Furthermore, the decision made by the TOPSIS method varies according to the selected ideal and non-ideal solutions. Therefore, to fairly compare the algorithms, the ideal and non-ideal solutions provided by the previous studies are used in the respective case studies. The results of the proposed algorithms are compared with variants of the well-known genetic algorithm and the particle swarm optimization algorithm in the respective case studies; Ahmadi *et al.*[2,3] employed the non-dominated sorting genetic algorithm (NSGAII), and Dai *et al.*[9] employed the multi-objective particle swarm optimization algorithm (MOPSO). The proposed algorithms are coded in MATLABR20015a and computations are performed by using a PC with 3.70-GHz Intel(R) Core i3–6100 CPU with 4GB of RAM. In the computational experiments, the algorithm parameters are kept constant for all the case studies and are presented in Table I. Sections IV A, IV B, and IV C present the multi-objective optimization case studies considered and the computational result analysis related to the respective case studies.

TABLE I. The algorithm parameters used in computational experiments of all case studies.

Parameter	Algorithm values		
	Jaya	MTPG Jaya	AMTPG Jaya
Population size (*N*)	100	100	100
Initial teams (*NT*)	…	4	2
Maximum movement iterations (*MaxMI*)	…	20	25
Maximum function evaluations (*MaxFevs*)	10 000	10 000	10 000

A. SDSHE case study 1

The multi-objective optimization problem considered in this case was formulated by Ahmadi *et al.*[3] for determining the optimal design parameters which simultaneously optimize the output power (P), thermal efficiency (η_m), and rate of entropy generation (σ) of an SDSHE system. The design equations based on the finite time thermodynamic analysis were formulated by Ahmadi *et al.*[3]

In the thermodynamic analysis of the SDSHE system, an SDSHE with the finite time regenerative process, regenerative heat loss, conductive thermal bridging loss, and finite heat transfer rate is considered to obtain the power output, thermal efficiency, and entropy generated. The entropy generation is a minimization function while the output power and the thermal efficiency are maximization functions. The decision variables and their constraints are presented in Table II. Let n be the number of moles of the working fluid, C_v the specific heat capacity of the working fluid during the regenerative process, R the universal gas constant, λ the ratio of volume during expansion and compression, M_1 the regenerative time constant at the heating region, M_2 the regenerative time constant at the cooling region, T_{H1} and T_{H2} the heat source temperature before and after heat transferred to the working fluid during the isothermal expansion, and T_{L1} and T_{L2} the heat sink temperature before and after heat transferred from the working fluid during isothermal compression, then the power output of a solar dish Stirling system is given by the following equation:

$$P = \frac{nR(T_h - T_c)\ln\lambda}{\frac{nRT_h\ln\lambda + nC_v(1-\varepsilon_R)(T_h - T_c)}{C_H\varepsilon_R(T_{H1} - T_h) + \zeta C_H\varepsilon_H\left(T_{H1}^4 - T_h^4\right)} + \frac{nRT_c\ln\lambda + nC_v(1-\varepsilon_R)(T_h - T_c)}{C_L\varepsilon_L(T_c - T_{L1})} + \left(\frac{1}{M1} + \frac{1}{M2}\right)(T_h - T_c)}. \quad (16)$$

Now, let Q_L be the net heat absorbed by the heat sink, Q_H the net heat released by the heat source, T_{Havg} and T_{Lavg} the average temperatures of the heat source and sink, η_t the thermal efficiency of the Stirling engine, and η_s the thermal efficiency of the dish collector, then the rate of entropy generation (σ) and thermal efficiency (η_m) of the system are given by the following equations, respectively,

$$\sigma = \frac{1}{t}\left(\frac{Q_L}{T_{L_{avg}}} - \frac{Q_H}{T_{H_{avg}}}\right), \quad (17)$$

$$\eta_m = \eta_s\eta_t, \quad (18)$$

$$\eta_t = \frac{nR(T_h - T_c)\ln\lambda}{nRT_h\ln\lambda + nC_v(1-\varepsilon_R)(T_h - T_c) + 0.5K_0\{(2-\varepsilon_H)T_{H1} - (2-\varepsilon_L)T_{L1} + (\varepsilon_H T_h - \varepsilon_L T_c)\}t}, \quad (19)$$

TABLE II. The decision variables considered for case study-1.[3]

Decision variable	Constraints
Regenerator effectiveness (ε_R)	$0.4 \le \varepsilon_R \le 0.9$
High-temperature heat exchanger effectiveness (ε_H)	$0.4 \le \varepsilon_H \le 0.8$
Low-temperature heat exchanger effectiveness (ε_L)	$0.4 \le \varepsilon_L \le 0.8$
Heat capacitance rate of the heat source (C_H)	$300 \le C_H \le 1800$
Heat capacitance rate of the heat sink (C_L)	$300 \le C_L \le 1800$
Working fluid temperature during isothermal expansion (T_h)	$800 \le T_h \le 1000$
Working fluid temperature during isothermal compression (T_c)	$400 \le T_c \le 510$

$$\eta_s = \eta_0 - \frac{1}{IC}\left[h\left(T_{\mathrm{H_{avg}}} - T_0\right) + \varepsilon\delta\left(T^4_{\mathrm{H_{avg}}} - T^4_0\right)\right], \qquad (20)$$

where T_0 is the ambient temperature, C is the collector concentrating ratio, ε is the emissivity factor of the collector, h is the convection heat transfer coefficient, I is the solar irradiance, δ is the Stefan-Boltzmann constant, and η_0 is the collector optical efficiency. The characteristics of the solar-dish Stirling engine system taken are the same as given by Ahmadi *et al.*[3] Those are as follows:

$$I = 1000\mathrm{Wm^{-2}},\ \varepsilon = 0.9,\ K_0 = 2.5\mathrm{WK^{-1}},$$
$$C_v = 15\,\mathrm{Jmol^{-1}k^{-1}},\quad C = 1300,\quad \eta_0 = 0.9,\quad n = 1\mathrm{mol},$$
$$\lambda = 2,\quad \zeta = 2\times10^{-10},\quad R = 4.3\,\mathrm{Jmol^{-1}K^{-1}},\quad T_{H1} = 1300\mathrm{K},$$
$$T_{L1} = 290\mathrm{K},\quad T_0 = 288\,\mathrm{K},\quad h = 20\,\mathrm{Wm^{-2}K^{-1}},$$
$$\delta = 5.67\times10^{-8}\mathrm{WK^{-4}m^{-2}},\quad (1/M_1 + 1/M_2) = 2\times10^{-5}\mathrm{sK^{-1}}.$$

Ahmadi *et al.*[3] solved this multi-objective optimization problem using NSGAII and reported three Pareto optimal solutions. These three solutions are documented based on the similarity to the ideal solutions calculated by employing TOPSIS, LINMAP, and Fuzzy Bellman-Zadeh decision-making methods. The number of function evaluations taken by the NSGAII is 400 000. The function evaluations taken by the proposed algorithms are 10 000. In the present work, each Pareto-frontier achieved by Jaya, MTPG Jaya, and AMTPG Jaya algorithms identified the best solution based on the similarity to an ideal solution using the TOPSIS technique and compared with those reported for the NSGAII.

In the TOPSIS selection process, the ideal solutions for the output power, thermal efficiency, and rate of entropy generation are taken to be 70 kW, 40%, and 20 W/K, respectively. Similarly, the nonideal solutions for the output power, thermal efficiency, and rate of entropy generation are taken to be 10 kW, 32%, and 120 W/K, respectively. The Pareto-frontier obtained by Jaya, MTPG Jaya, and AMTPG Jaya algorithms is shown in Fig. 4. Here, an observation can be made that the AMTPG Jaya algorithm obtained a more scattered Pareto-frontier when compared to that of MTPG Jaya and Jaya algorithms; this

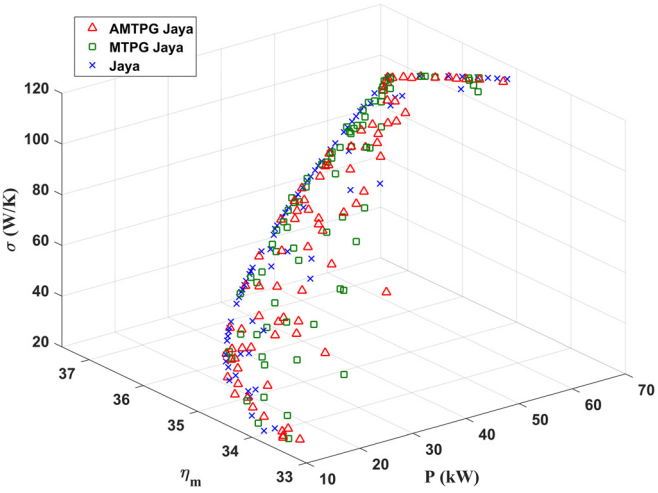

FIG. 4. The Pareto-frontier obtained by the proposed algorithms for case study-1.

indicates the efficiency of the proposed algorithm in exploring and exploiting the search space.

Furthermore, among the reported solutions identified a Pareto optimal solution relatively near to ideal solution using the TOPSIS method. The Pareto optimal solutions obtained for case study-1 by the AMTPG Jaya algorithm are presented in Table III. The output power obtained by the AMTPG Jaya algorithm is varied from 8.11 kW to 70.17 kW, the thermal efficiency of the system by the AMTPG Jaya algorithm is varied from 31.65% to 36.51%, and the entropy generation is varied from 22.60 W/K–138.98 W/K.

The computational results of the simultaneous three objective optimization are presented in Table IV. The Pareto optimal solutions of different algorithms are shown in Fig. 5. The TOPSIS decision-making method employed in this work is explained using the computational data presented in Table IV. Here for a three objective optimization problem, six alternatives have been presented in Table IV. The normalized values of the objective values corresponding to the respective alternatives can be calculated using Eq. (14), respectively. To calculate the normalized objective values, ideal and nonideal solutions are also considered. The normalized values are presented in Table V. By using these normalized values, the distances of the Pareto optimal solutions from ideal and nonideal solutions using Eqs. (12) and (13) are calculated, respectively.

After calculating, the distances are presented in Table V. Now using Eq. (16), the similarity index values are calculated and presented in Table V. Here, an observation can be made that the solution of the AMTPG Jaya algorithm has the highest relative similarity index when compared to that of the other solutions reported. Also, the optimal solution reported for the AMTPG Jaya algorithm has 0.05%, 0.65%, 1.32%, 3.17%, and 6.44% more similarity index to the ideal solution when compared to that of MTPG Jaya, Jaya, and NSGAII (TOPSIS, LINMAP, and Fuzzy Bellman-Zadeh) solutions, respectively. Furthermore, the output power obtained by the AMTPG Jaya algorithm solution is better, which is increased by 63%, 57%, and 23% when compared to those of the solutions reported by the NSGAII (Fuzzy, LINMAP, and TOPSIS), respectively. The thermal efficiency

TABLE III. Pareto optimal solutions (*1–100*) of the AMTPG Jaya algorithm for case study-1.

Sl. No	η_m (%)	P (kW)	σ (W/K)	ε_R	ε_H	ε_L	C_H	C_L	T_h	T_c
1	31.72	8.11	22.60	0.89161	0.40278	0.40840	300.89	300.16	998.53	401.00
2	31.65	70.17	138.98	0.89924	0.79870	0.79977	1799.95	1799.98	999.98	507.58
3	36.51	61.19	106.38	0.9000	0.79998	0.8000	1799.4	1799.9	999.7	400.0
4	36.02	31.98	57.87	0.90000	0.80000	0.79439	300.35	1204.14	999.95	400.16
5	36.32	48.32	85.76	0.90000	0.77746	0.78151	1799.88	1165.35	1000.0	400.03
6	35.77	33.71	61.55	0.89806	0.80000	0.80000	434.50	964.36	999.52	403.68
7	34.94	28.97	57.19	0.89376	0.76918	0.71272	1081.16	599.80	999.88	411.13
8	35.40	34.79	66.28	0.89900	0.49779	0.76383	554.22	1359.55	999.98	400.01
9	36.18	37.75	67.40	0.90000	0.79972	0.79853	339.89	1688.16	999.87	400.03
10	32.06	69.81	136.69	0.89877	0.79638	0.79977	1799.98	1799.99	999.98	498.12
11	36.10	50.10	89.77	0.90000	0.65460	0.80000	1081.41	1530.95	999.45	400.00
12	35.31	43.06	79.28	0.89745	0.78908	0.78216	934.00	1028.84	999.96	417.81
13	35.80	55.59	99.48	0.89764	0.79889	0.79952	1799.97	1395.30	999.97	411.02
14	34.18	67.63	124.09	0.90000	0.80000	0.80000	1800.00	1799.71	999.59	453.60
15	35.85	27.62	50.55	0.90000	0.80000	0.80000	300.62	825.76	998.92	400.29
16	35.79	57.19	101.97	0.89867	0.78306	0.79997	1076.39	1799.96	999.95	412.69
17	34.37	66.22	122.29	0.89757	0.77443	0.79976	1799.99	1799.99	999.99	444.48
18	32.68	25.21	50.11	0.89942	0.76090	0.79948	599.62	385.08	999.73	469.93
19	36.17	44.95	80.25	0.89830	0.79384	0.79953	1799.97	1008.59	999.98	400.22
20	35.55	21.65	40.57	0.90000	0.80000	0.80000	820.05	384.35	999.89	400.16
21	34.98	19.86	39.50	0.89997	0.65439	0.72390	818.99	383.08	999.97	403.09
22	35.86	54.57	98.78	0.89865	0.76226	0.76452	1002.09	1799.99	999.99	409.54
23	35.18	64.83	116.98	0.89899	0.79131	0.79236	1799.98	1800.00	999.78	429.11
24	36.03	53.41	97.18	0.89605	0.75199	0.77498	1247.50	1634.49	999.95	400.11
25	35.82	52.17	92.81	0.89941	0.79719	0.79980	936.48	1530.13	999.98	412.74
26	34.36	16.64	32.68	0.89994	0.80000	0.79984	300.26	300.26	999.02	418.84
27	35.66	28.29	51.88	0.90000	0.80000	0.80000	1444.97	496.81	999.36	405.60
28	36.27	42.60	76.01	0.89999	0.79604	0.77931	442.33	1799.62	999.97	400.00
29	34.76	15.18	30.17	0.90000	0.72076	0.80000	300.00	300.00	999.91	400.36
30	34.44	13.68	28.98	0.89659	0.78379	0.68472	300.03	300.01	999.67	400.02
31	35.26	19.10	36.60	0.90000	0.76326	0.80000	1026.66	320.76	997.61	400.00
32	32.41	69.57	134.82	0.89878	0.79824	0.79989	1799.97	1799.98	999.40	490.53
33	35.36	44.98	82.50	0.89763	0.78889	0.78691	1413.14	982.65	997.77	417.05
34	33.76	67.86	126.41	0.89934	0.78285	0.79961	1799.97	1799.99	999.95	461.29
35	32.95	69.10	131.31	0.89980	0.79485	0.79997	1786.49	1799.98	1000.0	480.20
36	35.38	28.80	54.36	0.90000	0.55425	0.80000	1800.00	535.17	999.78	400.48
37	34.81	65.52	119.41	0.89864	0.79524	0.79221	1799.98	1788.51	999.81	437.14
38	35.90	50.82	91.00	0.89986	0.79846	0.77439	1799.98	1198.52	1000.0	411.28
39	36.39	59.14	103.56	0.89935	0.79436	0.79937	1734.59	1689.93	1000.0	400.96
40	36.23	46.57	82.80	0.89865	0.79284	0.79997	557.74	1799.98	999.97	400.02
41	36.09	41.20	73.95	0.90000	0.71834	0.80000	442.25	1800.00	1000.0	400.00
42	34.25	12.66	27.64	0.90000	0.67368	0.63021	300.00	300.07	999.26	400.00
43	34.06	65.66	121.45	0.89892	0.79288	0.79994	1799.99	1680.28	999.95	454.17
44	35.40	41.56	75.83	0.89781	0.79718	0.79912	576.79	1200.90	999.33	416.04
45	34.99	15.51	30.36	0.90000	0.80000	0.80000	300.33	300.02	999.46	400.00
46	35.37	22.01	41.56	0.89925	0.77644	0.80000	1799.38	360.07	999.98	402.64
47	33.46	67.98	128.43	0.89754	0.78566	0.80000	1799.96	1799.97	1000.0	465.59
48	36.45	60.48	105.42	0.89986	0.79841	0.79937	1632.78	1799.98	999.97	401.13
49	35.83	63.21	111.99	0.89903	0.79452	0.79927	1799.96	1799.96	999.99	414.16

TABLE III. (*Continued.*)

Sl. No	η_m (%)	P (kW)	σ (W/K)	ε_R	ε_H	ε_L	C_H	C_L	T_h	T_c
50	35.84	47.35	84.96	0.89868	0.77563	0.80000	728.93	1471.01	999.57	408.39
51	36.47	59.78	104.15	0.90000	0.79577	0.80000	1528.10	1799.62	999.94	400.64
52	32.76	69.37	132.60	0.89979	0.79563	0.79916	1799.98	1800.00	999.99	484.33
53	36.06	62.82	110.31	0.89991	0.79712	0.79954	1799.97	1799.86	999.83	410.45
54	34.84	23.53	49.03	0.89662	0.53401	0.62273	1798.68	534.78	1000.00	400.05
55	33.87	33.98	64.40	0.89936	0.79772	0.79918	1800.00	509.69	999.65	450.37
56	34.88	24.86	49.43	0.89682	0.62277	0.72681	1244.99	486.54	999.68	406.26
57	33.13	68.70	130.50	0.89840	0.79345	0.79969	1800.00	1799.95	999.97	474.28
58	34.80	22.48	44.76	0.89910	0.51680	0.75152	1799.50	406.44	999.09	403.10
59	35.86	52.79	95.58	0.89860	0.63934	0.79950	1798.99	1394.70	999.86	403.09
60	33.33	68.69	129.28	0.89954	0.79359	0.79968	1799.97	1799.99	999.99	471.70
61	34.65	13.41	28.26	0.90000	0.80000	0.65133	300.66	300.00	998.49	400.07
62	35.14	17.69	34.48	0.89999	0.75631	0.77607	300.03	385.10	1000.00	400.10
63	34.90	16.50	34.15	0.89994	0.72713	0.64751	1798.32	320.30	997.07	400.03
64	35.12	19.64	37.96	0.90000	0.68812	0.80000	1798.94	320.12	996.47	400.18
65	32.51	69.45	134.08	0.89906	0.79316	0.79981	1800.00	1799.95	999.96	488.76
66	33.24	11.23	26.10	0.90000	0.40000	0.63919	300.04	300.19	993.51	400.00
67	36.15	39.98	73.66	0.90000	0.80000	0.70099	1799.91	934.44	1000.00	401.73
68	36.29	61.89	108.30	0.89979	0.79774	0.79921	1799.97	1799.97	999.03	404.64
69	36.05	57.91	103.48	0.89795	0.78491	0.78463	1288.37	1799.97	999.99	405.63
70	35.29	18.31	35.01	0.90000	0.80000	0.80000	300.00	385.63	1000.00	400.16
71	34.48	23.28	48.18	0.89580	0.51380	0.68749	1244.95	486.27	999.73	406.24
72	35.65	63.92	113.53	0.89937	0.79446	0.79934	1800.00	1799.98	999.96	419.01
73	36.16	62.14	109.23	0.89925	0.79387	0.79952	1799.99	1799.99	999.97	406.78
74	35.47	38.26	69.99	0.90000	0.70003	0.80000	445.61	1382.91	999.36	412.27
75	36.21	47.03	83.11	0.90000	0.79456	0.79976	1632.21	1082.58	999.60	402.93
76	36.16	52.61	94.09	0.89956	0.79364	0.76923	850.00	1799.97	996.93	404.32
77	34.91	34.24	64.78	0.89770	0.63852	0.79623	560.23	923.02	999.96	416.47
78	32.68	9.67	24.50	0.89640	0.44360	0.49869	300.00	300.03	994.78	400.03
79	33.62	9.47	23.23	0.89995	0.77474	0.41326	300.02	300.47	999.97	401.17
80	36.43	61.32	106.92	0.89992	0.79397	0.79833	1799.96	1799.96	999.97	401.49
81	35.63	39.21	72.56	0.90000	0.51867	0.80000	1108.81	1009.18	999.96	400.00
82	36.00	38.96	71.84	0.89781	0.78364	0.74293	890.04	1010.40	999.96	400.02
83	33.97	11.96	27.15	0.89492	0.77013	0.57698	300.04	300.05	1000.00	400.01
84	35.61	50.65	90.44	0.90000	0.80000	0.80000	748.15	1588.51	998.92	418.02
85	36.19	57.82	102.49	0.89755	0.79994	0.79997	1258.99	1799.98	999.97	402.37
86	35.37	64.25	115.58	0.89776	0.79767	0.79919	1799.99	1799.95	999.96	422.97
87	33.54	10.93	26.44	0.89953	0.57519	0.46004	599.29	306.16	997.06	400.81
88	35.89	39.95	72.92	0.89778	0.79807	0.77427	553.35	1238.22	999.34	403.71
89	33.92	22.89	46.49	0.90000	0.80000	0.68514	361.93	496.54	998.86	440.74
90	35.54	38.27	71.75	0.89848	0.77941	0.72514	445.27	1381.98	999.16	411.41
91	33.61	9.19	22.72	0.90000	0.80000	0.40000	300.00	300.55	997.97	400.00
92	33.30	9.98	24.65	0.89442	0.70766	0.46515	300.02	300.03	998.99	400.01
93	33.52	11.88	27.13	0.89733	0.50330	0.64125	300.03	300.01	999.36	400.05
94	33.48	10.53	25.47	0.89258	0.77642	0.49201	300.02	300.76	999.14	400.09
95	34.63	25.15	50.42	0.89815	0.45009	0.74234	1444.55	495.73	999.97	405.96
96	35.51	63.95	114.44	0.89831	0.79365	0.79964	1800.00	1799.96	999.97	420.33
97	35.94	37.89	70.03	0.89706	0.79110	0.75144	738.65	1015.46	999.99	400.03

TABLE III. (*Continued.*)

Sl. No	η_m (%)	P (kW)	σ (W/K)	ε_R	ε_H	ε_L	C_H	C_L	T_h	T_c
98	33.47	10.39	24.98	0.89947	0.58422	0.49977	300.37	300.14	999.01	400.01
99	35.11	18.08	35.00	0.89828	0.80000	0.79959	949.91	300.63	999.68	400.92
100	35.09	22.48	49.29	0.89818	0.63615	0.41803	442.65	976.69	999.95	400.04

TABLE IV. Pareto optimal solutions of different algorithms obtained for case study-1. NSGAII results are available in Ahmadi *et al.*[3] The results in the bold figure indicate a better value. SI—Relative similarity index to the ideal solution.

Method	ε_R	ε_H	ε_L	C_H	C_L	T_h	T_c	η_m (%)	P (kW)	σ (W/K)	SI
AMTPG Jaya-TOPSIS	0.9	0.79998	0.8	1799.36	1799.91	999.69	400	36.51	61.19	106.38	**0.50904**
MTPG Jaya-TOPSIS	0.9	0.8	0.8	1800	1800	999.79	400.86	36.48	61.34	106.71	0.50878
Jaya-TOPSIS	0.9	0.8	0.8	1800	1800	1000	410.23	36.08	**62.86**	110.19	0.50573
NSGAII-TOPSIS	0.9	0.8	0.8	1424	1252	996.9	400.5	**36.56**	49.64	87.47	0.50241
NSGAII-LINMAP	0.9	0.8	0.8	1413	823	996.7	400.5	36.36	38.86	**69.5**	0.49340
NSGAII-Fuzzy	0.9	0.8	0.8	1410	774	996.7	400.5	36.33	37.37	70	0.47825

of the solutions reported by the proposed algorithms is consistent with the NSGAII. The AMTPG Jaya algorithm solution has a lesser entropy generation when compared to that of Jaya and MTPG Jaya algorithms. For fair comparison with the previous studies, the ideal and nonideal solutions used are the same as those reported by Ahmadi *et al.*[3] However, if ideal and nonideal solutions are selected based on the Pareto optimal solutions of the AMTPG Jaya algorithm for TOPSIS decision-making, the best Pareto optimal solution obtained is better than the solutions reported in Table IV. According to this, the solution output power is 59.54 kW, the thermal efficiency is 36.5, and the rate of entropy generation is 103.6 W/K. In addition to the simultaneous optimization of three objectives, the two objective optimization is also carried to check the nature of these objectives. Figure 6 presents the Pareto-frontier for multi-objective optimization of the power output and thermal efficiency obtained by Jaya, MTPG Jaya, and AMTPG Jaya algorithms.

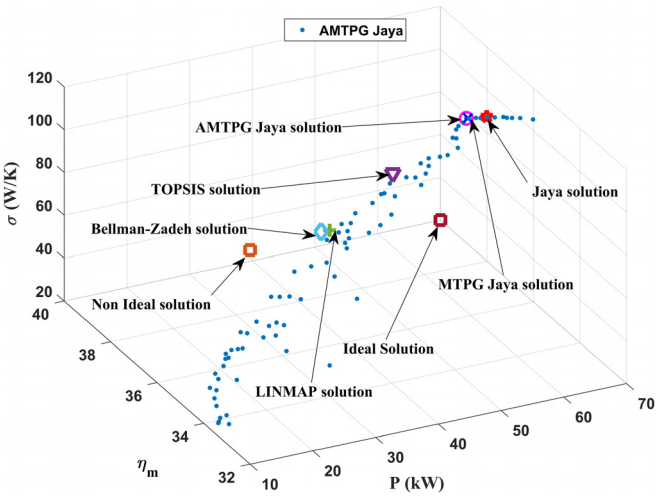

FIG. 5. The Pareto optimal solutions of different algorithms for case study-1.

Similarly, Fig. 7 presents the Pareto optimal front of simultaneous optimization of the power output and entropy generation. The Pareto optimal front of simultaneous optimization of thermal efficiency and entropy generation is shown in Fig. 8. An observation can be made here that the thermal efficiency and power output are conflicting objectives. Any change of design variables which increases thermal efficiency will result in a reduction of the power output. Similarly, any change of design variables which reduces the entropy generation will result in a reduction of the thermal efficiency and power output. Section IV B presents the second case study of the multi-objective optimization of an SDSHE system.

B. SDSHE case study 2

The multi-objective optimization problem considered in this case study is formulated by Dai *et al.*[9] for determining the optimal design parameters which simultaneously optimize the output power (P), efficiency (η), and ecological coefficient of performance ($ECOP$) of an SDSHE system. The design equations based on finite time thermodynamic analysis were formulated by Dai *et al.*[9] for a Stirling engine. Dai *et al.*[9] developed an analytical model by considering conductive thermal bridging loss, finite heat transfer rate, and compensating the regenerative heat loss by supplying heat from a heat source, to obtain the power output, efficiency, and $ECOP$.

The three objective functions considered in this case study are maximization functions. The decision variables and their constraints are presented in Table VI. Let n be the number of moles of the working fluid, C_v the constant volume specific heat capacity of the working fluid during the regenerative processes, R the universal gas constant, λ the ratio of volume, k_1 the rate of temperature change at the heating region, k_2 the rate of temperature change at the cooling region, T_H the heat source temperature, T_L the heat sink temperature, α_h the

TABLE V. Sample values calculated for case study-1 results using the TOPSIS method.

	Normalized values					
Method	P (kW)	η_m (%)	σ (W/K)	d_i^{ideal}	$d_i^{nonideal}$	SI
AMTPG Jaya-TOPSIS	0.414156	0.355151	0.410900	0.3406308	0.3531792	0.50904
MTPG Jaya-TOPSIS	0.415171	0.354860	0.412174	0.3417330	0.3539520	0.50878
Jaya-TOPSIS	0.425459	0.350969	0.425616	0.3537618	0.3619591	0.50573
NSGAII-TOPSIS	0.335982	0.355638	0.337858	0.2966914	0.2995648	0.50241
NSGAII-LINMAP	0.263019	0.353692	0.268448	0.2867624	0.2792897	0.49340
NSGAII-Fuzzy	0.252934	0.353401	0.270379	0.2955478	0.2709063	0.47825

convective heat transfer coefficient during isothermal expansion, α_c the convective heat transfer coefficient during isothermal compression, μ_{2-3} the inadequate regeneration coefficient during the isochoric heat addition process, and μ_{4-1} inadequate regeneration coefficient during the isochoric heat rejection process, then the power output of a solar dish Stirling system is given by the following equation:

$$P = \frac{nR(T_h - T_c)\ln\lambda}{t}, \tag{21}$$

where t is the Stirling cycle time, given by the following equation:

$$t = \left(\frac{1-\mu_{2-3}}{k_1} + \frac{1-\mu_{4-1}}{k_2}\right)(T_h - T_c) + \frac{nRT_h\ln\lambda}{\alpha_h(T_H - T_h)} + \frac{nRT_c\ln\lambda}{\alpha_c(T_l - T_L)} + \frac{mC_v}{\alpha_h}\ln\frac{T_H - \mu_{2-3}T_c - (1-\mu_{2-3})T_h}{T_H - T_h} + \frac{mC_v}{\alpha_c}\ln\frac{\mu_{4-1}T_h - T_L + (1-\mu_{4-1})T_c}{T_c - T_L}. \tag{22}$$

Let α_{leak} be the coefficient of heat leak and σ the entropy generated, then the following equations give the efficiency and ECOP:

$$\eta = \frac{nR(T_h - T_c)\ln\lambda}{\alpha_{leak}(T_H - T_L)t + \mu_{2-3}mC_v(T_h - T_c) + nRT_h\ln\lambda}, \tag{23}$$

$$\mathrm{ECOP} = \frac{nR(T_h - T_c)ln\lambda}{T_0\sigma}, \tag{24}$$

$$\sigma = \left(\frac{\alpha_{leak}(T_H - T_L)t + \mu_{4-1}mC_v(T_h - T_c) + nRT_l\ln\lambda}{T_L} - \frac{\alpha_{leak}(T_H - T_L)t + \mu_{2-3}mC_v(T_h - T_c) + nRT_h\ln\lambda}{T_H}\right). \tag{25}$$

The characteristics of the Stirling engine system taken are same as given by the Dai *et al.*[9] Those are as follows:

$$m = 4\,\mathrm{g}, \quad \mu_{2-3} = 0.3, \quad \mu_{4-1} = 0.2, \quad C_v = 3.214\,\mathrm{Jg^{-1}k^{-1}},$$
$$k_1 = k_2 = 5000\frac{\mathrm{K}}{\mathrm{s}}, \quad T_0 = 300\,\mathrm{K}, \quad n = 1\mathrm{mol},$$
$$\lambda = 2, \quad R = 8.314\,\mathrm{Jmol^{-1}K^{-1}}, \quad \alpha_c = \alpha_h = 1000\mathrm{W/(K\,s)},$$
$$\alpha_{leak} = 12\,\mathrm{W/(K\,s)}.$$

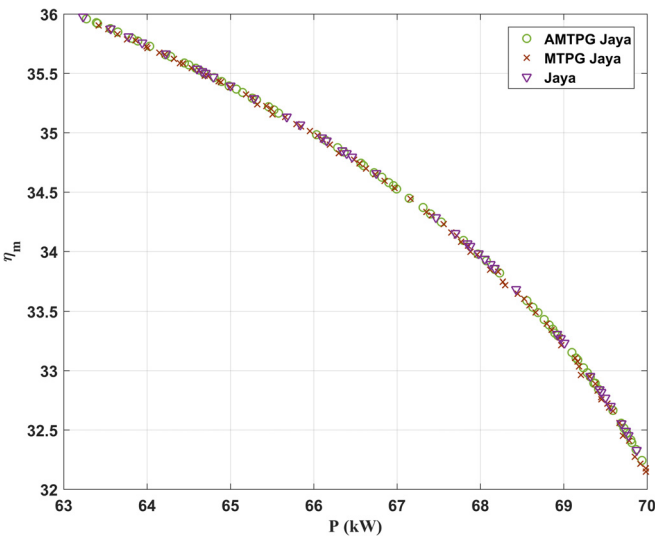

FIG. 6. The Pareto optimal solutions for the two objective optimization (P-η_m) for case study-1.

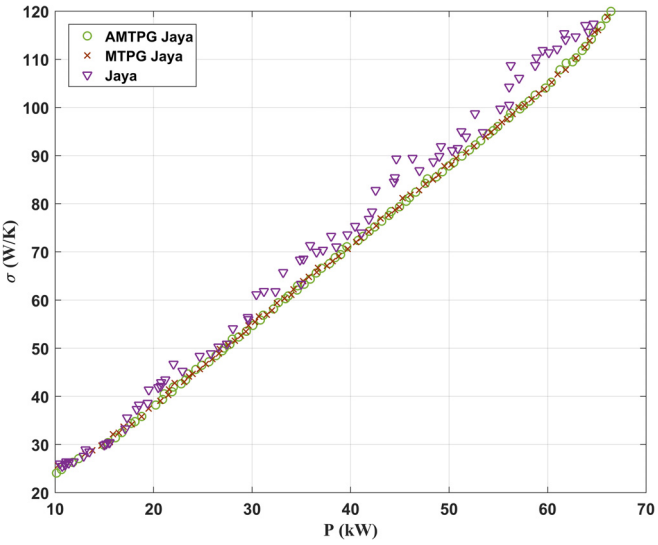

FIG. 7. The Pareto optimal solutions for two objective optimization (P-σ) for case study-1.

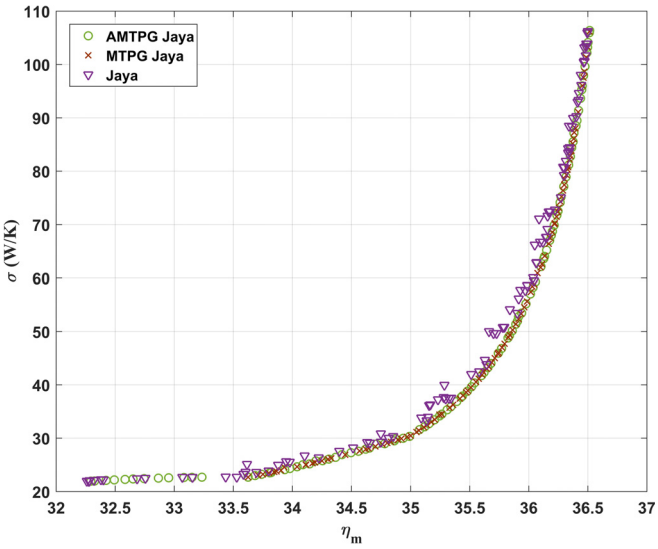

FIG. 8. The Pareto optimal solutions for two objective optimization (η_m-σ) for case study-1.

Dai *et al.*[9] solved this multi-objective optimization problem using MOPSO and reported one Pareto optimal solution by employing the TOPSIS decision-making method. The number of function evaluations taken by the MOPSO algorithm for this case study was unspecified. Hence, the proposed algorithms are executed for 10 000 function evaluations. For each algorithm, the Pareto-frontier has identified the best solution based on the similarity to an ideal solution using the TOPSIS technique and compared with that of MOPSO. In the TOPSIS selection process, the ideal solutions for output power, efficiency, and *ECOP* are taken as 16 kW, 36% and 1.1, respectively. Similarly, the nonideal solutions for the output power, efficiency, and *ECOP* are taken to be 8 kW, 26%, and 0.6, respectively. Furthermore, among the reported solutions, a Pareto optimal solution relatively nearer to the ideal solution is identified using the TOPSIS method. The Pareto optimal solutions obtained for case study-2 by the AMTPG Jaya algorithm are presented in Table VII. The output power obtained by the AMTPG Jaya algorithm is varied from 10.55 kW to 14.60 kW, the efficiency of the system by the AMTPG Jaya algorithm is varied from 28.47% to 33.49%, and ECOP is varied from 0.63506 to 1.0935. Figure 9 presents the Pareto-frontiers obtained by Jaya, MTPG Jaya, and AMTPG Jaya algorithms for case study-2. Similar to case study-1, it can be observed here that the AMTPG Jaya algorithm obtained a more scattered Pareto-frontier when compared to MTPG Jaya and Jaya algorithms. The Pareto-frontiers of MTPG Jaya and Jaya

TABLE VI. The decision variables considered for case study-2.[9]

Decision variable	Constraints
Heat source temperature (T_H)	$1000 \leq T_H \leq 1200$
Heat sink temperature (T_L)	$280 \leq T_L \leq 300$
Working fluid temperature during isothermal expansion (T_h)	$600 \leq T_h \leq 1000$
Working fluid temperature during isothermal compression (T_c)	$300 \leq T_c \leq 600$

TABLE VII. Pareto optimal solutions of AMTPG Jaya algorithm for case study-2.

Sl. No.	T_h	T_l	T_H	T_L	P (kW)	η (%)	*ECOP*	Sl. No.	T_h	T_l	T_H	T_L	P (kW)	η (%)	*ECOP*
1	874.4	455.4	1200	280	14.60	28.47	0.64	51	999.9	326.3	1152.8	286.04	12.28	33.32	0.92
2	999.9	325.9	1135.0	280	12.33	33.50	0.91	52	854.3	356.4	1029.4	300	12.21	32.24	1.03
3	896.7	340.4	1000.0	300	10.87	32.75	1.09	53	880.8	341.6	1000.0	300	11.13	32.71	1.09
4	900.0	322.5	1000.0	290.24	10.56	32.95	1.04	54	921.7	382.5	1132.1	300	13.40	32.02	0.93
5	896.9	434.2	1200.0	280	14.57	29.72	0.69	55	965.1	371.3	1200.0	280	14.07	32.48	0.82
6	891.1	442.9	1200.0	280	14.59	29.29	0.67	56	868.7	337.5	1013.7	289.71	11.81	32.89	1.02
7	944.9	401.5	1200.0	280	14.37	31.48	0.77	57	989.4	327.1	1123.0	283.18	12.16	33.42	0.93
8	885.0	443.4	1200.0	280	14.59	29.16	0.66	58	999.9	354.0	1200.0	280	13.69	33.07	0.85
9	929.5	407.0	1200.0	280	14.43	31.12	0.75	59	856.6	361.2	1000.0	300	11.97	32.25	1.06
10	875.9	452.7	1200.0	280	14.60	28.61	0.64	60	943.7	399.0	1162.5	286.78	13.97	31.71	0.83
11	886.9	449.4	1200.0	280	14.60	28.96	0.66	61	858.1	352.6	1000.0	300	11.73	32.44	1.07
12	906.5	433.5	1200.0	280	14.56	29.90	0.70	62	886.0	373.9	1093.0	300	13.07	31.98	0.96
13	891.4	437.6	1200.0	280	14.58	29.49	0.68	63	977.1	348.6	1193.8	300	12.92	32.74	0.94
14	950.4	396.9	1198.5	280	14.31	31.68	0.78	64	935.3	385.8	1200.0	280	14.29	31.81	0.79
15	906.0	427.2	1200.0	280	14.55	30.12	0.71	65	937.4	368.0	1167.0	280.42	13.88	32.45	0.84
16	875.2	448.5	1200.0	280	14.60	28.77	0.65	66	999.9	345.1	1146.8	291.41	12.60	33.21	0.95
17	960.3	414.2	1200.0	280	14.37	31.29	0.76	67	896.2	342.5	1035.6	300	11.56	32.77	1.06
18	909.4	425.5	1200.0	280	14.54	30.23	0.71	68	999.9	378.0	1200.0	300	13.57	32.55	0.92
19	927.0	383.4	1200.0	283.79	14.22	31.77	0.80	69	987.0	338.8	1142.2	280	12.89	33.39	0.90

TABLE VII. (*Continued.*)

Sl. No.	T_h	T_l	T_H	T_L	P (kW)	η (%)	*ECOP*	Sl. No.	T_h	T_l	T_H	T_L	P (kW)	η (%)	*ECOP*
20	932.9	413.7	1200.0	280	14.45	30.96	0.74	70	912.3	330.5	1031.4	283.89	11.67	33.27	0.99
21	889.4	325.7	1000.0	287.82	11.02	33.09	1.03	71	907.0	330.3	1013.5	283.06	11.43	33.24	1.00
22	977.9	419.9	1200.0	298.72	14.08	31.35	0.85	72	974.5	336.8	1086.8	287.01	11.88	33.27	0.97
23	914.4	408.8	1200.0	280	14.47	30.86	0.74	73	997.4	380.7	1200.0	294.63	13.74	32.50	0.89
24	930.7	420.8	1200.0	280	14.48	30.71	0.73	74	983.6	375.4	1133.3	295.07	13.01	32.68	0.95
25	895.4	437.6	1200.0	280	14.58	29.57	0.68	75	887.1	338.7	1000.0	294.92	11.20	32.87	1.07
26	898.6	332.1	1000.0	296.52	10.68	32.83	1.07	76	919.2	366.9	1057.8	297.49	12.40	32.58	1.01
27	901.8	429.0	1200.0	280	14.56	29.99	0.70	77	986.0	363.6	1139.7	299.85	12.78	32.87	0.98
28	920.0	419.4	1200.0	280	14.50	30.60	0.73	78	905.0	333.9	1021.6	284.86	11.66	33.20	1.00
29	857.4	368.1	1000.0	300	12.09	32.09	1.04	79	901.1	361.0	1075.7	298.15	12.64	32.51	0.99
30	891.9	411.3	1199.0	280	14.50	30.44	0.72	80	999.9	334.6	1200.0	280	13.29	33.30	0.86
31	959.6	393.7	1200.0	280	14.27	31.86	0.79	81	964.4	380.8	1171.8	289.96	13.75	32.35	0.88
32	908.4	421.4	1200.0	280	14.53	30.35	0.72	82	981.3	389.0	1200.0	299.54	13.81	32.17	0.90
33	942.3	397.7	1200.0	292.56	14.16	31.56	0.83	83	976.8	377.8	1200.0	280	14.09	32.43	0.82
34	876.7	446.7	1200.0	280	14.60	28.87	0.65	84	884.5	332.9	1001.8	286.32	11.47	33.10	1.02
35	960.1	326.3	1126.1	280.61	12.53	33.40	0.91	85	977.6	344.1	1110.3	300	11.92	33.02	1.01
36	928.3	425.0	1200.0	285.36	14.44	30.54	0.75	86	848.9	374.2	1000.0	300	12.27	31.83	1.02
37	909.1	342.9	1013.7	299.22	11.10	32.81	1.08	87	902.7	355.2	1013.6	300	11.52	32.66	1.07
38	967.3	383.6	1200.0	280	14.17	32.20	0.81	88	980.4	352.1	1167.6	280	13.47	33.11	0.87
39	950.9	428.5	1200.0	298.29	14.23	30.77	0.82	89	931.2	360.3	1128.1	297.03	13.02	32.61	0.96
40	899.1	331.1	1000.0	283.21	11.29	33.18	1.01	90	968.7	335.3	1162.2	280	13.13	33.28	0.88
41	953.3	344.5	1058.4	300	11.34	32.92	1.05	91	987.0	348.9	1200.0	287.81	13.43	32.99	0.89
42	918.2	333.4	1044.1	280	12.05	33.33	0.96	92	882.6	336.0	1018.2	280.54	12.09	33.15	0.97
43	999.9	366.8	1200.0	280	13.86	32.84	0.84	93	999.9	332.3	1139.5	280	12.58	33.48	0.91
44	970.9	380.3	1200.0	280	14.13	32.32	0.81	94	945.6	354.0	1160.4	280.18	13.61	32.85	0.86
45	968.4	395.8	1200.0	300	13.93	31.89	0.89	95	999.9	332.2	1189.7	280	13.14	33.36	0.87
46	891.6	353.3	1000.0	300	11.36	32.63	1.08	96	999.9	348.8	1166.1	280	13.26	33.26	0.88
47	925.0	428.5	1200.0	289.83	14.40	30.39	0.76	97	942.9	355.7	1100.0	280	13.04	33.01	0.90
48	969.6	358.3	1144.2	300	12.83	32.84	0.98	98	974.1	359.9	1168.7	280	13.63	32.92	0.86
49	872.2	361.6	1000.0	300	11.82	32.38	1.07	99	926.5	322.8	1069.0	280	12.00	33.41	0.95
50	965.6	366.4	1200.0	280	14.01	32.59	0.83	100	999.9	326.7	1165.6	280	12.73	33.45	0.89

algorithms are clustered and dense when compared to that of the AMTPG Jaya algorithm; this signifies the exploring capability of the proposed algorithm.

The computational results of simultaneous three objective optimization are presented in Table VIII. The Pareto optimal solutions of different algorithms are shown in Fig. 10. Here, an observation can be made that the solution of the AMTPG Jaya algorithm has the highest relative similarity index when compared to the other solutions reported. Also, the optimal solutions reported for the Jaya, MTPG Jaya, and AMTPG Jaya algorithms have 1.12%, 1.63% and 1.89% better similarity index when compared to that of MOPSO solution. Furthermore, output power obtained by AMTPG Jaya algorithm solution is better, which is increased by 4.39%, 4.5%, and 9.11% when compared to those of the solutions reported by the MTPG Jaya, Jaya, and MOPSO respectively. The thermal efficiency of the solutions reported by the proposed algorithms is consistent with MOPSO algorithm. The MTPG Jaya algorithm attained better efficiency when compared to that of Jaya, AMTPG Jaya and MOPSO algorithms. The ECOP of MOPSO algorithm solution is better than others.

In addition to the three objective simultaneous optimization, the two objective optimization was also carried out to check the nature of these objectives. Figure 11 presents the Pareto-frontier for multi-objective optimization of the power output and efficiency obtained by Jaya, MTPG Jaya, and AMTPG Jaya algorithms, respectively. The contradicting nature of power output and efficiency can be observed from Fig. 11, any change in the design variable which increases the efficiency will result in a reduction of power output. The power output varied from 12.7 kW to 14.61 kW and efficiency varied from 28.4% to 33.5%.

Similarly, Fig. 12 presents the Pareto optimal front of simultaneous optimization of power output and *ECOP*. The power output and *ECOP* are also conflicting in nature. In this optimization, the power output varied from 10.81 kW to 14.67 kW, and *ECOP* varied between 0.647 and 1.093. Figure 13 shows the Pareto optimal front of

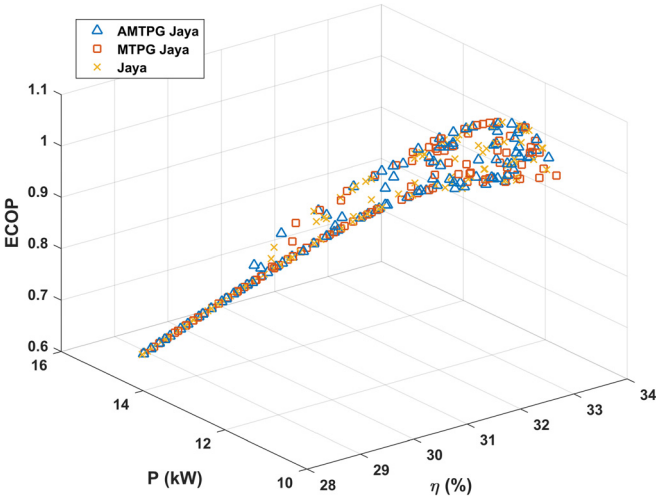

FIG. 9. The Pareto-frontier obtained by the proposed algorithms for case study-2.

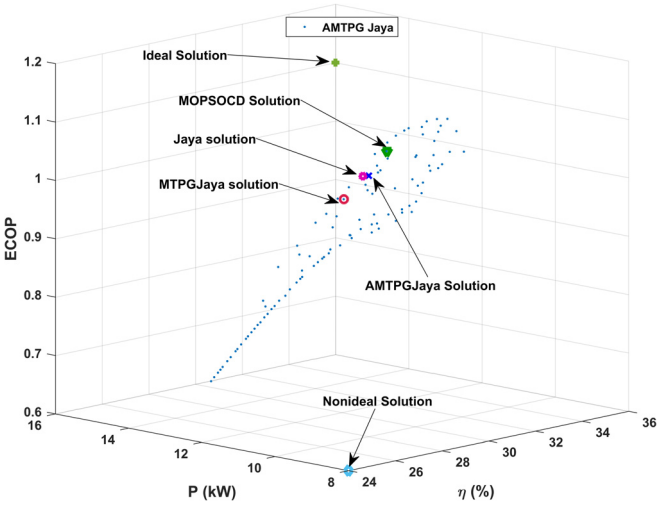

FIG. 10. The Pareto optimal solutions of different algorithms for case study-2.

simultaneous optimization of efficiency and *ECOP*. An observation can be made here that efficiency and *ECOP* are conflicting objectives. In this optimization, the efficiency varied from 32.74% to 33.5% and *ECOP* varied between 0.913 and 1.091. Section IV C presents a multi-objective optimization case study of the Stirling heat pump system.

C. Case study of the Stirling heat pump

The multi-objective optimization problem considered in this case study is formulated by Ahmadi *et al.*[2] for determining the optimal design parameter combination that simultaneously optimizes the input power (P), the heating coefficient of performance (COP_H), and the heating load (R_H) of an irreversible Stirling heat pump system. The design equations for a Stirling heat pump system based on finite time thermodynamic analysis were formulated by Ahmadi *et al.*[2] considering both internal and external irreversibilities to obtain the power input, the coefficient of performance in heating (COP_H), and the heating load.

The power input of the Stirling heat pump needs to be minimized while the COP_H and R_H need to be maximized. The decision variables and their constraints are presented in Table IX. Let n be the number of moles of the working fluid, C_v the specific heat capacity of the working fluid, R the universal gas constant, λ the ratio of volume during expansion and compression, ϕ the internal irreversibility parameter, α the proportionality constant, ε_R the regenerator effectiveness, and T_h the hot side temperature, the hot side temperature varies from T_{H1} to T_{H2} and cold side temperature varies from T_{L1} to T_{L2}, then the analytical

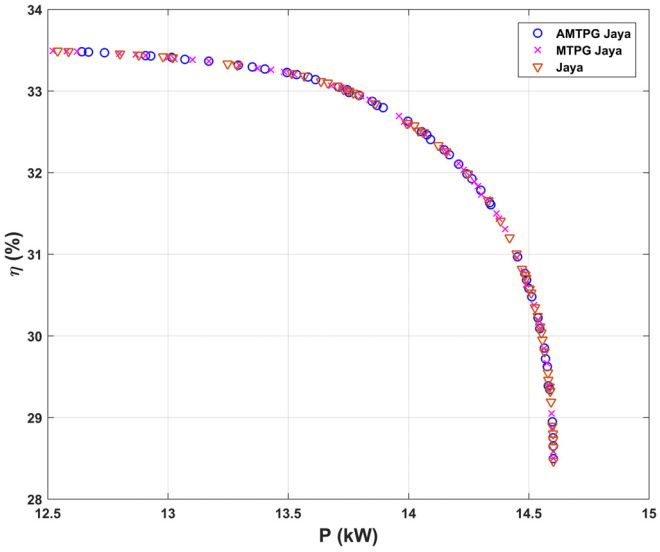

FIG. 11. The Pareto optimal solutions for two objective optimization (P-η) for case study-2.

TABLE VIII. Pareto optimal solutions of different algorithms obtained for case study-2. The results of MOPSO are available in Dai *et al.*[9] The results in the bold figure indicate a better value. SI—Relative similarity index to the ideal solution.

Method	T_h	T_l	T_H	T_L	P (kW)	η (%)	*ECOP*	*SI*
AMTPG Jaya-TOPSIS	999.9	378.0	1200	300	**13.57**	32.545	0.92472	**0.67334**
MTPG Jaya-TOPSIS	971.0	367.8	1142.3	300	13.004	**32.721**	0.97044	0.67163
Jaya-TOPSIS	950.7	378.1	1114.0	300	12.99	32.449	0.97201	0.66825
MOPSO-TOPSIS	917	362.3	1070.4	300.0	12.44	32.62	**1.02**	0.66084

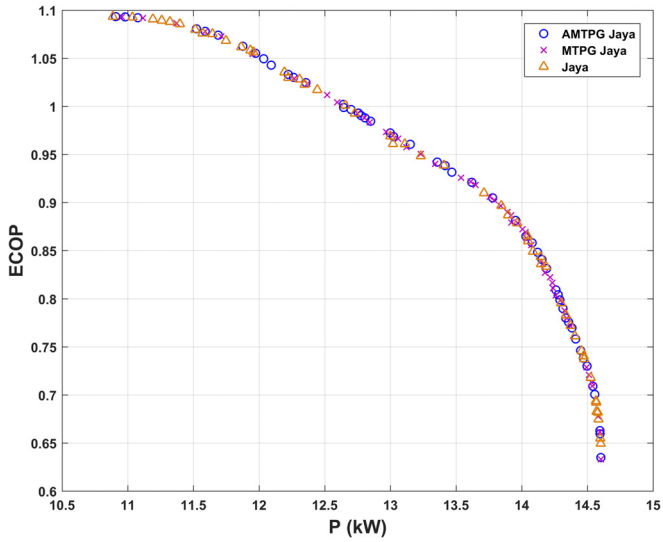

FIG. 12. The Pareto optimal solutions for two objective optimization (*P-ECOP*) for case study-2.

equations of power input, R_H, and COP_H are given by the following equations:

$$P = (\chi - \phi)/\left(\frac{\chi}{C_H\varepsilon_H(\chi T_c - T_{H1})} + \frac{\phi}{C_L\varepsilon_L(T_{L1} - T_c)} + \frac{2\alpha}{n\mathrm{Rln}\lambda}(\chi - 1)\right), \tag{26}$$

$$R_H = \left(\chi - \frac{C_v(1-\varepsilon_R)(\chi-1)}{\mathrm{Rln}\lambda}\right)/\left(\frac{\chi}{C_H\varepsilon_H(\chi T_c - T_{H1})} + \frac{\phi}{C_L\varepsilon_L(T_{L1} - T_c)} + \frac{2\alpha}{n\mathrm{Rln}\lambda}(\chi - 1)\right), \tag{27}$$

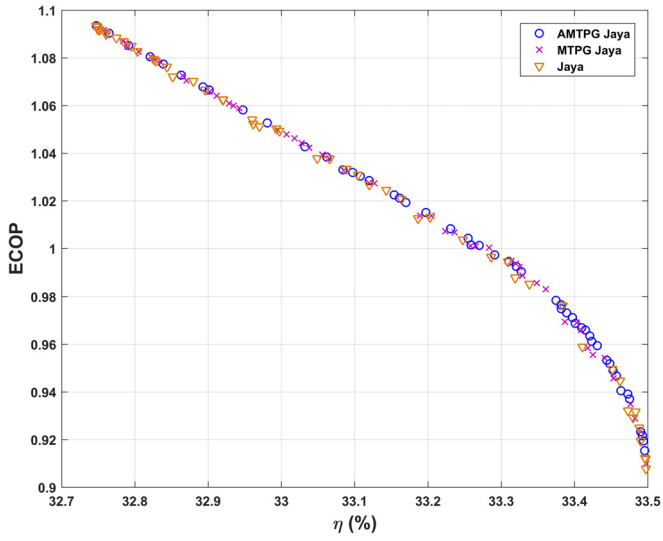

FIG. 13. The Pareto optimal solutions for two objective optimization (η-*ECOP*) for case study-2.

TABLE IX. The decision variables considered for the case study of the Stirling heat pump.[2]

Decision variable	Constraints
Temperature ratio T_h/T_c (χ)	$1.3 \le \chi \le 1.4$
High-temperature heat exchanger effectiveness (ε_H)	$0.5 \le \varepsilon_H \le 0.8$
Low-temperature heat exchanger effectiveness (ε_L)	$0.5 \le \varepsilon_L \le 0.8$
Heat capacitance rate of the heat source (C_H)	$600 \le C_H \le 1000$
Heat capacitance rate of the heat sink (C_L)	$600 \le C_L \le 1000$

$$\mathrm{COP}_H = \left(\chi - \frac{C_v(1-\varepsilon_R)(\chi-1)}{\mathrm{Rln}\lambda}\right)/(\chi - \phi), \tag{28}$$

where, $\chi = T_h/T_c$.

The characteristics of the Stirling heat pump system considered in the present work are the same as those taken by Ahmadi *et al.*[2] These are as follows:

$$T_{H1} = 330\,\mathrm{K}, \quad T_{L1} = 290 \quad \mathrm{K}, C_v = 15 \quad \mathrm{Jmol^{-1}k^{-1}},$$
$$\varepsilon_R = 0.9, \phi = 0.8, \quad \alpha = 10^{-5}\,\mathrm{sK^{-1}}, \quad n = 1\mathrm{mol},$$
$$\lambda = 2, \quad R = 4.3\,\mathrm{Jmol^{-1}K^{-1}}$$

Ahmadi *et al.*[2] solved this multi-objective optimization problem using NSGAII and reported three Pareto optimal solutions. These three solutions are documented based on the similarity to the ideal solutions calculated by employing TOPSIS, LINMAP, and Fuzzy Bellman-Zadeh decision-making methods. The number of function evaluations taken by the NSGAII for this case study was unspecified. The proposed algorithms are evaluated for 10 000 function evaluations.

In the present work, each Pareto-frontier achieved by Jaya, MTPG Jaya, and AMTPG Jaya algorithms identified the best solution based on the similarity to an ideal solution using the TOPSIS technique and compared with those reported for the NSGAII. In the TOPSIS selection process, the ideal solutions for P, R_H, and COP_H are taken to be 0.5 kW, 14 kW, and 2.3, respectively. Similarly, the non-ideal solutions for P, R_H, and COP_H are taken to be 7 kW, 0.1 kW, and 2, respectively. Finally, among the reported solutions identified a Pareto optimal solution relatively near to ideal solution using the TOPSIS method.

The Pareto optimal solutions obtained for the Stirling heat pump case study by the AMTPG Jaya algorithm are presented in Table X. In the Pareto-frontier obtained by the AMTPG Jaya algorithm for three objective simultaneous optimization, the power input is varied from 0.0721 kW to 6.806 kW, the COP_H of the system is varied from 1.99782 to 2.29804, and R_H is varied between 0.1659 kW and 13.599 kW. The Pareto-frontier obtained by Jaya, MTPG Jaya, and AMTPG Jaya algorithms is shown in Fig. 14. Here, an observation can be made that the AMTPG Jaya algorithm obtained a more scattered Pareto-frontier when compared to that of MTPG Jaya and Jaya algorithms; this connotes that the AMTPG Jaya algorithm could exploit the search space effectively when compared to that of Jaya and MTPG Jaya algorithms.

TABLE X. Pareto optimal solutions (*1–100*) of the AMTPG Jaya algorithm for the heat pump case study.

Sl. No.	P (kW)	R_H (kW)	COP_H	ε_H	ε_L	T_c	χ	C_H	C_L
1	5.44	10.88	1.99782	0.50000	0.80000	267.8	1.40000	998.2	999.0
2	0.07	0.17	2.29804	0.50000	0.80000	254.2	1.30000	801.8	918.3
3	6.81	13.60	1.99782	0.80000	0.80000	268.1	1.40000	997.7	975.7
4	2.66	6.11	2.29804	0.66222	0.50000	267.0	1.30000	998.9	976.9
5	6.27	12.58	2.00697	0.69512	0.77408	268.0	1.39637	998.9	999.1
6	4.94	10.16	2.05808	0.54405	0.74158	269.1	1.37685	997.9	998.8
7	4.87	9.92	2.03428	0.51042	0.71847	267.7	1.38577	998.3	975.2
8	4.35	9.63	2.21474	0.74228	0.79609	268.1	1.32424	998.8	976.5
9	5.16	10.83	2.10070	0.65048	0.78449	269.2	1.36152	998.7	998.5
10	4.15	9.00	2.16571	0.57651	0.79093	267.8	1.33964	998.3	976.6
11	4.97	10.40	2.09178	0.77950	0.58296	267.6	1.36466	998.7	999.4
12	1.87	4.17	2.23064	0.64775	0.52850	258.9	1.31943	800.1	852.7
13	2.95	6.75	2.28662	0.57919	0.65709	268.8	1.30319	998.9	998.5
14	1.18	2.41	2.04943	0.76437	0.73102	242.9	1.38006	756.3	686.1
15	5.77	11.54	1.99782	0.56728	0.80000	268.0	1.40000	998.5	976.3
16	6.00	11.98	1.99782	0.60661	0.80000	267.0	1.40000	998.7	975.4
17	1.14	2.36	2.07419	0.51092	0.66814	247.8	1.37095	604.3	640.3
18	1.04	2.34	2.25347	0.74311	0.75147	255.0	1.31268	817.4	913.2
19	0.88	2.00	2.26502	0.64337	0.64313	255.7	1.30934	803.4	898.3
20	1.28	2.84	2.21489	0.53343	0.63007	255.5	1.32420	826.1	837.7
21	3.66	8.07	2.20336	0.74282	0.64223	268.8	1.32774	800.1	999.8
22	0.79	1.74	2.19105	0.67049	0.55065	250.9	1.33157	777.0	742.5
23	4.10	8.84	2.15607	0.80000	0.50000	269.0	1.34278	997.3	998.9
24	4.61	9.82	2.13081	0.78678	0.71437	261.8	1.35117	944.0	977.8
25	3.09	6.93	2.24301	0.52587	0.67133	268.1	1.31576	997.3	998.1
26	0.74	1.61	2.17816	0.56328	0.53272	250.7	1.33565	741.6	691.0
27	2.05	4.46	2.17401	0.65845	0.64912	255.6	1.33697	800.0	813.7
28	0.30	0.61	2.04000	0.55453	0.54409	240.0	1.38360	641.9	730.5
29	1.49	3.11	2.08495	0.76231	0.71428	246.6	1.36709	725.3	768.1
30	1.34	3.07	2.29340	0.68321	0.50954	259.3	1.30129	831.5	832.3
31	2.52	5.42	2.14753	0.66362	0.65865	255.4	1.34559	869.1	805.7
32	0.83	1.75	2.11214	0.60659	0.64483	246.9	1.35754	682.2	789.3
33	3.91	8.79	2.24789	0.76328	0.73625	267.5	1.31432	997.9	975.5
34	0.69	1.47	2.11765	0.60015	0.54206	246.4	1.35564	756.3	660.5
35	5.49	10.97	1.99782	0.50744	0.80000	268.0	1.40000	999.1	998.8
36	0.63	1.36	2.16369	0.55030	0.54547	249.3	1.34030	728.2	716.9
37	0.20	0.42	2.12524	0.60155	0.52512	244.9	1.35305	632.2	667.7
38	1.19	2.70	2.27816	0.59276	0.57100	258.4	1.30558	814.0	815.5
39	0.39	0.86	2.20069	0.62359	0.61261	250.1	1.32856	703.8	630.9
40	6.43	12.85	1.99782	0.80000	0.80000	266.9	1.40000	858.6	986.3
41	0.11	0.23	2.13956	0.55934	0.60973	245.3	1.34824	715.7	707.1
42	3.44	7.85	2.28003	0.68461	0.69675	269.8	1.30505	999.5	976.6
43	3.68	8.26	2.24832	0.78820	0.58489	268.9	1.31419	998.1	976.6
44	1.15	2.38	2.07645	0.62266	0.51839	245.5	1.37014	778.8	656.4
45	0.87	1.90	2.19496	0.67736	0.53164	251.4	1.33035	782.2	744.8
46	2.71	6.23	2.29804	0.80000	0.50538	268.0	1.30000	955.2	799.7
47	0.44	1.00	2.27167	0.50000	0.80000	254.6	1.30743	802.5	917.5
48	3.29	7.57	2.29804	0.80000	0.80000	267.8	1.30000	859.8	984.6

TABLE X. (*Continued.*)

Sl. No.	P (kW)	R_H (kW)	COP_H	ε_H	ε_L	T_c	χ	C_H	C_L
49	1.37	3.07	2.23715	0.80000	0.50000	255.4	1.31749	802.5	804.3
50	0.96	2.05	2.14411	0.62919	0.64258	248.9	1.34672	788.7	625.7
51	3.12	7.17	2.29804	0.80000	0.50000	269.4	1.30000	998.1	999.9
52	3.86	8.31	2.15126	0.51440	0.73147	267.2	1.34436	999.9	976.6
53	0.13	0.27	2.03443	0.63037	0.67784	238.6	1.38572	786.2	800.3
54	0.51	1.09	2.13428	0.63266	0.64463	246.4	1.35000	797.6	786.4
55	0.32	0.73	2.27122	0.80000	0.80000	253.4	1.30756	806.2	884.7
56	3.88	8.34	2.15061	0.61298	0.76618	268.5	1.34457	800.0	976.7
57	1.50	3.17	2.11511	0.58723	0.51601	250.9	1.35652	706.3	757.5
58	2.34	5.38	2.29804	0.50000	0.50000	268.5	1.30000	998.5	998.8
59	1.24	2.83	2.28277	0.52327	0.80000	259.3	1.30427	832.2	832.6
60	1.64	3.49	2.12951	0.67988	0.72691	250.4	1.35161	798.0	716.1
61	0.29	0.61	2.12754	0.59656	0.56057	244.9	1.35228	998.0	998.7
62	6.58	13.14	1.99782	0.80000	0.75431	268.3	1.40000	997.6	976.4
63	1.48	3.10	2.09617	0.64833	0.62163	248.1	1.36311	787.8	609.3
64	3.28	7.54	2.29804	0.72360	0.80000	266.7	1.30000	999.0	998.9
65	1.56	3.48	2.23561	0.72345	0.74478	256.2	1.31795	801.1	945.7
66	0.71	1.58	2.23273	0.62160	0.54313	253.1	1.31881	806.1	885.0
67	2.55	5.85	2.29804	0.50000	0.62215	269.1	1.30000	998.7	977.4
68	0.21	0.43	2.09896	0.77407	0.54446	242.9	1.36213	760.2	682.0
69	4.87	9.91	2.03429	0.54354	0.71704	265.1	1.38577	947.9	980.1
70	2.07	4.76	2.29804	0.52217	0.80000	263.8	1.30000	952.1	998.8
71	1.90	4.37	2.29804	0.50000	0.50000	265.9	1.30000	858.3	984.3
72	0.51	1.18	2.28632	0.69112	0.71895	254.9	1.30327	906.4	857.5
73	1.70	3.91	2.29804	0.50000	0.69550	262.4	1.30000	943.3	977.1
74	6.76	13.50	1.99782	0.80000	0.80000	268.7	1.40000	998.3	975.6
75	2.15	4.93	2.29804	0.50000	0.73576	266.5	1.30000	858.9	984.4
76	0.58	1.23	2.11251	0.59758	0.64503	245.8	1.35741	685.3	691.6
77	1.80	4.13	2.29804	0.50000	0.50000	263.7	1.30000	947.1	979.8
78	2.24	5.15	2.29804	0.50000	0.50000	267.1	1.30000	999.9	998.2
79	6.66	13.30	1.99782	0.80000	0.77350	269.4	1.40000	999.3	997.9
80	1.65	3.79	2.29804	0.50000	0.72841	262.0	1.30000	945.1	977.5
81	3.50	8.03	2.29804	0.80000	0.71930	267.8	1.30000	997.4	976.1
82	0.87	1.90	2.17626	0.55765	0.64968	252.2	1.33625	612.7	656.5
83	1.51	3.46	2.29804	0.50000	0.65767	262.5	1.30000	827.3	859.4
84	2.21	5.08	2.29804	0.59366	0.80000	263.5	1.30000	944.2	977.9
85	1.47	3.09	2.09977	0.56788	0.65986	249.8	1.36184	692.0	753.7
86	6.62	13.23	1.99782	0.80000	0.75473	267.8	1.40000	999.2	976.4

The computational results of the simultaneous three objective optimization are presented in Table XI. The Pareto optimal solutions of different algorithms are compared in Fig. 15. Here, an observation can be made that, the solution of the AMTPG Jaya algorithm has the highest relative similarity index when compared to that of the other solutions reported. An observation can be made here that the COP_H variation is decidedly less in compared to the power input and heating load. Furthermore, the heating load of the AMTPG Jaya algorithm solution is more, which is increased by 4.5%, 0.4%, 11.3%, 8.2%, and 7.1% when compared to that of the solutions reported by MTPG Jaya, Jaya, and NSGAII (TOPSIS, LINMAP, and Fuzzy) algorithms, respectively. The heating coefficient of performance of the AMTPG Jaya algorithm solution increased by 0.15%, 0.18%, 0.22%, and 0.40% when compared to that of the solutions reported by Jaya and NSGAII (TOPSIS, LINMAP, and Fuzzy) algorithms, respectively. The MTPG Jaya algorithm attained the same COP_H as that of the AMTPG Jaya algorithm. In this case study, a best Pareto optimal solution has been identified based on the ideal and nonideal solutions selected from the

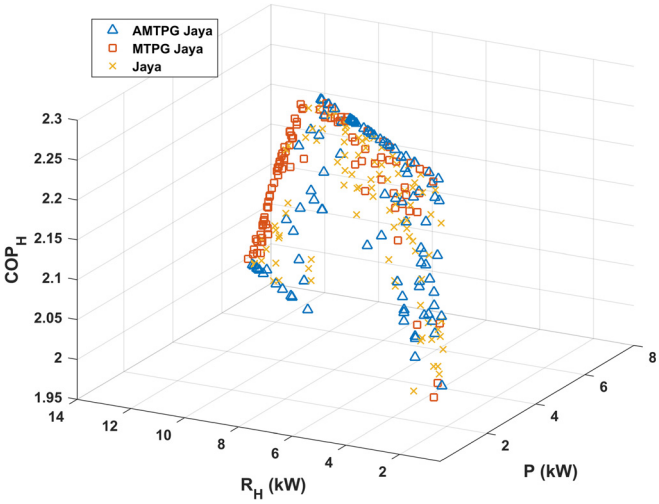

FIG. 14. The Pareto-frontier obtained by the proposed algorithms for the heat pump case study.

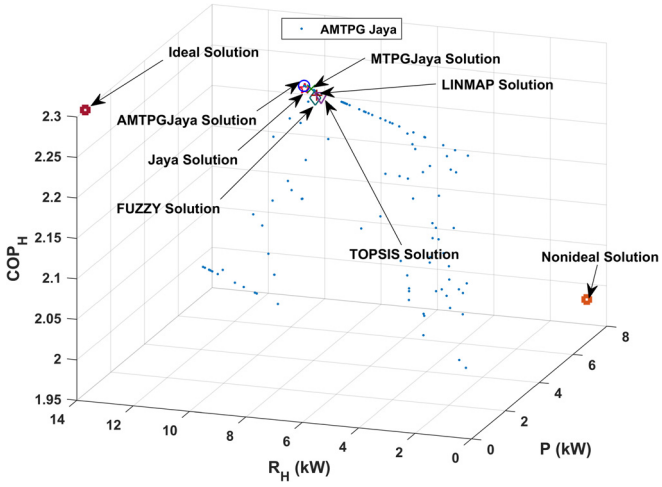

FIG. 15. The Pareto optimal solutions of different algorithms for the heat pump case study.

Pareto front of the AMTPG Jaya algorithm. According to that, the solution power input, heating load, and COP_H are 3.36 kW, 7.722 kW, and 2.298041, respectively.

In addition to the three objective simultaneous optimization, the two objective optimization was also carried out to check the nature of these objectives. Figure 16 presents the Pareto-frontier for multi-objective optimization of the power input and heating coefficient of performance obtained by Jaya, MTPG Jaya, and AMTPG Jaya algorithms. From Fig. 16, it can be observed that the Pareto optimal solutions of Jaya and MTPG Jaya are more crowded than those of the AMTPG Jaya algorithm.

Similarly, Fig. 17 shows the Pareto optimal front of simultaneous optimization of input power and COP_H. An observation can be made here that the input power and COP_H are conflicting objectives. Figure 18 presents the Pareto optimal front of simultaneous optimization of COP_H and R_H. The heating load and heating COP are also conflicting in nature. In this optimization, the heating load varied from 8.1 kW to 13.96 kW and COP_H varied between 1.98 and 2.298. Section V presents the conclusions of this work.

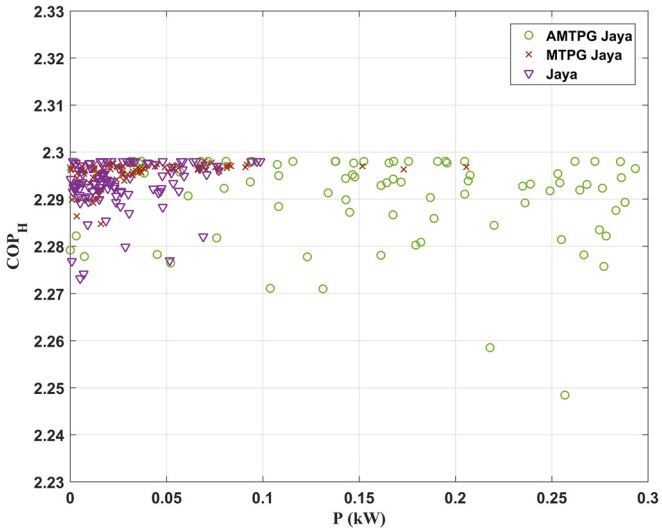

FIG. 16. The Pareto optimal solutions for two objective optimization (P-COP_H) for the heat pump case study.

TABLE XI. Pareto optimal solutions of different algorithms obtained for the heat pump case study. The results for NSGA-II are available in Ahmadi *et al.*[2] The results in the bold figure indicate a better value. SI—Relative similarity index to the ideal solution.

Method	ε_H	ε_L	T_c	X	C_H	C_L	P (kW)	R_H (kW)	COP_H	SI
AMTPG Jaya-TOPSIS	0.8	0.7	267.8	1.3	997.436	976.130	3.49628	**8.03458**	**2.29804**	**0.556**
MTPG Jaya-TOPSIS	0.6353	0.8	270	1.3	1000.0	1000.0	3.34557	7.68825	**2.29804**	0.555
Jaya-TOPSIS	0.8	0.6745	269.9	1.3009	999.992	919.358	3.48756	8.00279	2.29466	0.555
NSGAII-TOPSIS	0.7259	0.7896	268.1	1.3011	956.062	798.933	**3.14709**	7.21882	2.29381	0.554
NSGAII-LINMAP	0.7461	0.7555	267.8	1.3014	939.557	906.077	3.23860	7.42602	2.29297	0.554
NSGAII-Fuzzy	0.7429	0.7171	268.3	1.3025	937.105	927.633	3.27914	7.50534	2.28882	0.554

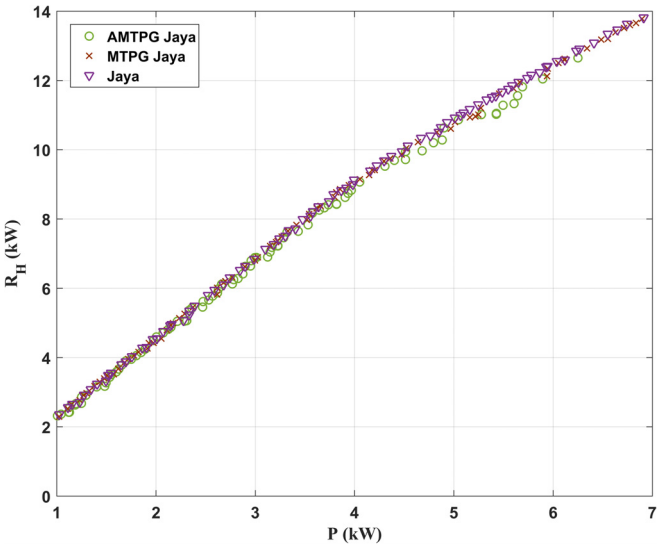

FIG. 17. The Pareto optimal solutions for two objective optimization (P-R_H) for the heat pump case study.

V. CONCLUSIONS

A multi-objective optimization variant of the Jaya algorithm called the AMTPG Jaya algorithm is proposed in this work. The proposed approach explores and exploits the search space by adapting multiple teams of a single population set guided by multiple movement equations. The proposed algorithm's performance has been investigated using two multi-objective optimization case studies of the SDSHE system and a multi-objective optimization case study of the Stirling heat pump. Furthermore, the TOPSIS decision-making method has been employed to compare the performance of the proposed algorithm with that of other algorithms reported in the literature.

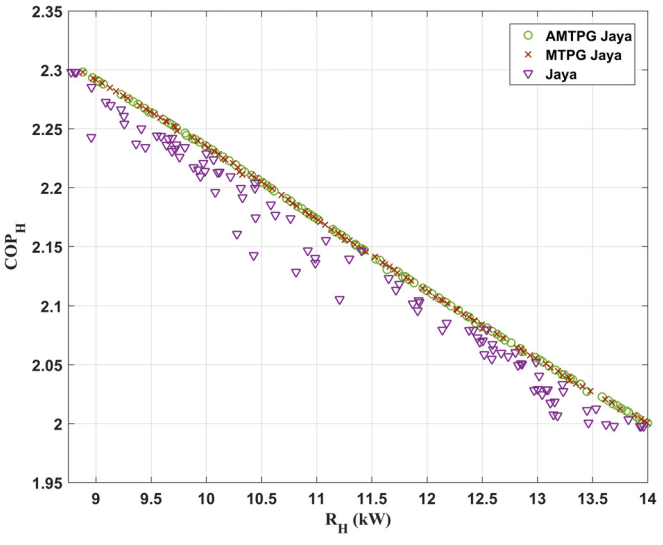

FIG. 18. The Pareto optimal solutions for two objective optimization (R_H-COP_H) for the heat pump case study.

- In SDSHE case study 1, the AMTPG Jaya algorithm attained a better Pareto optimal solution that has a 51% similarity index to the ideal solution. The similarity index of the AMTPG Jaya algorithm is 0.05%, 0.65%, 1.32%, 3.17%, and 6.43% higher when compared to that of MTPG Jaya, Jaya, TOPSIS, LINMAP, and Fuzzy Bellman-Zadeh solutions, respectively.
- In addition, the output power given by the AMTPG Jaya algorithm is 63%, 57%, and 23% more when compared to that of the solutions reported by the Fuzzy Bellman-Zadeh, LINMAP, and TOPSIS, respectively.
- In SDSHE case study 2, with 67% similarity index to the ideal solution, the AMTPG Jaya algorithm has obtained a better Pareto optimal solution which is 1.89%, 0.76%, and 0.25% higher when compared to the solutions of MOPSO, Jaya, and MTPG Jaya algorithms, respectively.
- The output power obtained by the AMTPG Jaya algorithm is better by 4.39%, 4.5%, and 9.11% when compared to the solutions reported by the MTPG Jaya, Jaya, and MOPSO algorithms, respectively.
- In the Stirling heat pump case study, the AMTPG Jaya algorithm has the highest relative similarity index (55.6%) when compared to that of the other solutions reported.
- The heating load and COP_H given by the AMTPG Jaya algorithm are higher. The heating load is increased by 4.5%, 0.40%, 11.3%, 8.2%, and 7.1%, and the COP_H is increased by 0%, 0.14%, 0.18%, 0.22%, and 0.40% when compared to the solutions reported by MTPG Jaya, Jaya, TOPSIS, LINMAP, and Fuzzy Bellman-Zadeh algorithms, respectively.

The computational results have shown that the Pareto-optimal solutions obtained by the proposed approach for all the multi-objective optimization case studies considered are superior to those achieved by the other algorithms.

REFERENCES

[1]M. H. Ahmadi, M. A. Ahmadi, A. Mellit, F. Pourfayaz, and M. Feidt, "Thermodynamic analysis and multi-objective optimization of the performance of solar dish Stirling engine by the centrality of entransy and entropy generation," Int. J. Electr. Power Energy Syst. **78**, 88–95 (2016).
[2]M. H. Ahmadi, M. A. Ahmadi, A. H. Mohammadi, M. Mehrpooya, and M. Feidt, "Thermodynamic optimization of Stirling heat pump based on multiple criteria," Energy Convers. Manage. **80**, 319–328 (2014).
[3]M. H. Ahmadi, A. H. Mohammadi, S. Dehghani, and M. A. Barranco-Jiménez, "Multi-objective thermodynamic-based optimization of the output power of solar dish-Stirling engine by implementing an evolutionary algorithm," Energy Convers. Manage. **75**, 438–445 (2013).
[4]M. H. Ahmadi, H. Sayyaadi, S. Dehghani, and H. Hosseinzade, "Designing a solar-powered Stirling heat engine based on multiple criteria: Maximized thermal efficiency and power," Energy Convers. Manage. **75**, 282–291 (2013).
[5]M. H. Ahmadi, H. Sayyaadi, and H. Hosseinzadeh, "Optimization of output power and thermal efficiency of solar-dish Stirling engine using finite time thermodynamic analysis," Heat Transfer - Asian Res. **44**, 347–376 (2015).
[6]R. Arora, S. C. Kaushik, and R. Kumar, "Multi-objective thermodynamic optimization of solar parabolic dish Stirling heat engine using NSGAII and decision making," Int. J. Renewable Energy Technol. **8**, 64–92 (2017).
[7]R. Arora, S. C. Kaushik, R. Kumar, and R. Arora, "Multi-objective thermo-economic optimization of solar parabolic dish Stirling heat engine with regenerative losses using NSGAII and decision making," Int. J. Electr. Power Energy Syst. **74**, 25–35 (2016).
[8]D. A. Blank, G. W. Davis, and C. Wu, "Power optimization of an endoreversible Stirling cycle with regeneration," Energy **19**, 125–133 (1994).

[9]D. Dai, F. Yuan, R. Long, Z. Liu, and W. Liu, "Performance analysis and multi-objective optimization of a Stirling engine based on MOPSOCD," Int. J. Therm. Sci. **124**, 399–406 (2018).
[10]K. Deb, A. Pratap, S. Agarwal, and T. Meyarivan, "A fast and elitist multiobjective genetic algorithm: NSGAII," IEEE Trans. Evol. Comput. **6**, 182–197 (2002).
[11]D. C. Du, H. H. Vinh, V. D. Trung, N. T. H. Quyen, and N. T. Trung, "Efficiency of Jaya algorithm for solving the optimization-based structural damage identification problem based on a hybrid objective function," Eng. Optim. **50**, 1233–1251 (2018).
[12]C. Duan, X. Wang, S. Shu, C. Jing, and H. Chang, "Thermodynamic design of Stirling engine using multi-objective particle swarm optimization algorithm," Energy Convers. Manage. **84**, 88–96 (2014).
[13]M. Hooshang, S. Toghyani, A. Kasaeian, R. A. Moghadam, and M. H. Ahmadi, "Enhancing and multi-objective optimizing of the performance of Stirling engine using third-order thermodynamic analysis," Int. J. Ambient Energy **39**, 382–391 (2018).
[14]S. C. Kaushik and S. Kumar, "Finite time thermodynamic analysis of endoreversible Stirling heat engine with regenerative losses," Energy **25**, 989–1003 (2000).
[15]S. C. Kaushik and S. Kumar, "Finite time thermodynamic evaluation of irreversible Ericsson and Stirling heat engines," Energy Convers. Manage. **42**, 295–312 (2001).
[16]T. Liao and J. Lin, "Optimum performance characteristics of a solar-driven Stirling heat engine system," Energy Convers. Manage. **97**, 20–25 (2015).
[17]P. D. Michailidis, "An efficient multi-core implementation of the Jaya optimization algorithm," Int. J. Parallel, Emergent Distrib. Syst. **34**, 288-320 (2017).
[18]M. R. Nazemzadegan, A. Kasaeian, S. Toghyani, M. H. Ahmadi, R. Saidur, and T. Ming, "Multi-objective optimization in a finite time thermodynamic method for dish-Stirling by branch and bound method and MOPSO algorithm," Front. Energy 1–17 (2018).
[19]Q. Niu, S. Ziyuan, and D. Hua, "An improved multi-objective bare-bones PSO for optimal design of solar dish Stirling engine systems," in *Advanced Computational Methods in Energy, Power, Electric Vehicles, and Their Integration: International Conference on Life System Modeling and Simulation, LSMS 2017 and International Conference on Intelligent Computing for Sustainable Energy and Environment*, Nanjing, China (2017), pp. 167–177.
[20]P. Ocłoń, P. Cisek, M. Rerak, D. Taler, R. V. Rao, A. Vallati, and M. Pilarczyk, "Thermal performance optimization of the underground power cable system by using a modified Jaya algorithm," Int. J. Therm. Sci. **123**, 162–180 (2018).
[21]V. Punnathanam and P. Kotecha, "Multi-objective optimization of Stirling engine systems using Front-based Yin-Yang-pair optimization," Energy Convers. Manage. **133**, 332–348 (2016).
[22]R. V. Rao, *Decision Making in the Manufacturing Environment: Using Graph Theory and Fuzzy Multiple Attribute Decision Making Methods*, *Springer Series in Advanced Manufacturing* (Springer-Verlag London Limited, 2007).
[23]R. V. Rao, https://sites.google.com/site/jayaalgorithm/ for Jaya-Algorithm; accessed 8 September 2015.
[24]R. V. Rao, "Jaya: A simple and new optimization algorithm for solving constrained and unconstrained optimization problems," Int. J. Ind. Eng. Comput. **7**, 19–34 (2016).
[25]R. V. Rao, *Jaya: An Advanced Optimization Algorithm and its Engineering Applications*, 1st ed. (Springer International Publishing AG, Part of Springer Nature, 2019).
[26]R. V. Rao and H. S. Keesari, "Multi-team perturbation guiding Jaya algorithm for optimization of wind farm layout," Appl. Soft Comput. J. **71**, 800–815 (2018).
[27]R. V. Rao, K. C. More, L. S. Coelho, and V. C. Mariani, "Multi-objective optimization of the Stirling heat engine through self-adaptive Jaya algorithm," J. Renewable Sustainable Energy **9**, 033703 (2017).
[28]R. V. Rao, K. C. More, J. Taler, and P. Ocłoń, "Dimensional optimization of a micro-channel heat sink using Jaya algorithm," Appl. Therm. Eng. **103**, 572–582 (2016).
[29]R. V. Rao and D. P. Rai, "Optimisation of welding processes using quasi-oppositional-based Jaya algorithm," J. Exp. Theor. Artif. Intell. **29**, 1099–1117 (2017).
[30]R. V. Rao, D. P. Rai, and J. Balic, "Multi-objective optimization of machining and micro-machining processes using non-dominated sorting teaching–learning-based optimization algorithm," J. Intell. Manuf. **29**, 1715–1737 (2016).
[31]R. V. Rao, D. P. Rai, J. Ramkumar, and J. Balic, "A new multi-objective Jaya algorithm for optimization of modern machining processes," Adv. Prod. Eng. Manage. **11**, 271–286 (2016).
[32]R. V. Rao and A. Saroj, "Economic optimization of shell-and-tube heat exchanger using Jaya algorithm with maintenance consideration," Appl. Therm. Eng. **116**, 473–487 (2017).
[33]R. V. Rao and A. Saroj, "Multi-objective design optimization of heat exchangers using elitist-Jaya algorithm," Energy Syst. **9**, 305–341 (2018).
[34]R. V. Rao, A. Saroj, P. Ocłoń, J. Taler, and D. Taler, "Single- and multi-objective design optimization of plate-fin heat exchangers using Jaya algorithm," Heat Trans. Eng. **39**, 13–14 (2018).
[35]A. Sharma, S. K. Shukla, and A. K. Rai, "Finite time thermodynamic analysis and optimization of solar-dish Stirling heat engine with regenerative losses," Therm. Sci. **15**, 995–1009 (2011).
[36]A. R. Tavakolpour-Saleh, S. H. Zare, and H. Badjian, "Multi-objective optimization of Stirling heat engine using gray wolf optimization algorithm," Int. J. Eng. **30**, 895–903 (2017).
[37]D. G. Thombare and S. K. Verma, "Technological development in the Stirling cycle engines," Renewable Sustainable Energy Rev. **12**, 1–38 (2008).
[38]I. Tlili, Y. Timoumi, and S. B. Nasrallah, "Thermodynamic analysis of the Stirling heat engine with regenerative losses and internal irreversibilities," Int. J. Engine Res. **9**, 45–56 (2008).
[39]S. Toghyani, A. Kasaeian, and M. H. Ahmadi, "Multi-objective optimization of Stirling engine using non-ideal adiabatic method," Energy Convers. Manage. **80**, 54–62 (2014).
[40]S. Wang, R. V. Rao, P. Chen, Y. Zhang, A. Liu, and L. Wei, "Abnormal breast detection in mammogram images by feed-forward neural network trained by Jaya algorithm," Fundam. Inf. **151**, 191–211 (2017).
[41]W. Warid, H. Hizam, N. Mariun, and N. I. Abdul-Wahab, "Optimal power flow using the Jaya algorithm," Energies **9**, 678 (2016).
[42]L. Yaqi, H. Yaling, and W. Weiwei, "Optimization of solar-powered Stirling heat engine with finite-time thermodynamics," Renewable Energy **36**, 421–427 (2011).
[43]K. Yu, J. J. Liang, B. Y. Qu, X. Chen, and H. Wang, "Parameters identification of photovoltaic models using an improved JAYA optimization algorithm," Energy Convers. Manage. **150**, 742–753 (2017).
[44]Y. Zhang, X. Yang, C. Cattani, R. V. Rao, S. Wang, and P. Phillips, "Tea category identification using a novel fractional Fourier entropy and Jaya algorithm," Entropy **18**, 77 (2016).